Eur. Phys. J. A (2013) **49**: 94
DOI 10.1140/epja/i2013-13094-7

The European Physical Journal A

Regular Article – Experimental Physics

Mass yield distributions of fission products from photo-fission of ^{238}U induced by 11.5–17.3 MeV bremsstrahlung

H. Naik[1,a], Frédérick Carrel[2], G.N. Kim[3], Frédéric Laine[2], Adrien Sari[2], S. Normand[4], and A. Goswami[1]

[1] Radiochemistry Division, Bhabha Atomic Research Centre, Mumbai - 400085, India
[2] SAPHIR Facility, CEA, Saclay, LIST, Gif-sur-Yvette F-91191, France
[3] Department of Physics, Kyungpook National University, Daegu 702-701, Republic of Korea
[4] Laboratory of Sensors and Elctronics Architectures CEA, Saclay, Gif-sur-Yvette 91191, France

Received: 31 March 2013 / Revised: 3 June 2013
Published online: 18 July 2013 –
Communicated by J. Äystö

Abstract. The yields of various fission products in the 11.5, 13.4, 15.0 and 17.3 MeV bremsstrahlung-induced fission of ^{238}U have been determined by recoil catcher and an off-line γ-ray spectrometric technique using the electron linac, SAPHIR at CEA, Saclay, France. The mass yield distributions were obtained from the fission product yields using charge-distribution corrections. The peak-to-valley (P/V) ratio, average light mass ($\langle A_{\mathrm{L}}\rangle$) and heavy mass ($\langle A_{\mathrm{H}}\rangle$) and average number of neutrons ($\langle v\rangle$) in the bremsstrahlung-induced fission of ^{238}U at different excitation energies were obtained from the mass yield data. From the present and literature data in the $^{238}\mathrm{U}(\gamma,f)$ and $^{238}\mathrm{U}(n,f)$ reactions at various energies, the following observations were obtained: i) The mass yield distributions in the $^{238}\mathrm{U}(\gamma,f)$ reaction at various energies of the present work are double-humped, similar to those of the $^{238}\mathrm{U}(n,f)$ reaction of comparable excitation energy. ii) The yields of fission products for $A = 133$–134, $A = 138$–140, and $A = 143$–144 and their complementary products in the $^{238}\mathrm{U}(\gamma,f)$ reaction are higher than other fission products due to the nuclear structure effect. iii) The yields of fission products for $A = 133$–134 and their complementary products are slightly higher in the $^{238}\mathrm{U}(\gamma,f)$ than in the $^{238}\mathrm{U}(n,f)$, whereas for $A = 138$–140 and 143–144 and their complementary products are comparable. iv) With excitation energy, the increase of yields of symmetric products and the decrease of the peak-to-valley (P/V) ratio in the $^{238}\mathrm{U}(\gamma,f)$ reaction is similar to the $^{238}\mathrm{U}(n,f)$ reaction. v) The increase of $\langle v\rangle$ with excitation energy is also similar between the $^{238}\mathrm{U}(\gamma,f)$ and $^{238}\mathrm{U}(n,f)$ reactions. However, it is surprising to see that the $\langle A_{\mathrm{L}}\rangle$ and $\langle A_{\mathrm{H}}\rangle$ values with excitation energy behave entirely differently from the $^{238}\mathrm{U}(\gamma,f)$ and $^{238}\mathrm{U}(n,f)$ reactions.

1 Introduction

The study of mass and charge distribution in low-energy photon- and neutron-induced fission of actinides provides information about the effect of nuclear structure and dynamics of descent from saddle to scission [1,2]. This is because in the photon-induced fission the mass and charge of the compound nucleus is the same as that of the target nucleus, whereas in the neutron-induced fission, the compound nucleus mass increases by only one unit. It is a well-known fact that the mass distributions [1,2] in the photon- and neutron-induced fission of medium-Z actinides (*e.g.*, U to Cf) are asymmetric with double hump, whereas for light-Z actinides (*e.g.*, Ac, Th, Pa) they are asymmetric with triple hump [1,2]. However, with the increase of excitation energy and Z of the actinide, the mass distribution changes from asymmetric to symmetric and the effect of the nuclear structure decreases. Among these, the photon- and neutron-induced fissions of Th, U and Pu are important for the understanding of basic fission phenomena and for their application in various types of reactors. The photon- and neutron-induced fission of ^{232}Th and ^{233}U are of interest for the advanced heavy water reactor (AHWR) [3,4] and accelerator-driven subcritical system (ADSS) [5–10]. On the other hand photon- and neutron-induced fissions of ^{235,238}U and ^{239}Pu are important in conventional light and heavy water reactor and fast reactor [11–15]. Besides this, the bremsstrahlung- and neutron-induced fissions of ^{232}Th and ^{238}U above the fission barrier to the end of the giant dipole resonance (GDR) region is interesting from the point of view of the nuclear structure effect such as the role of shell closure proximity and the even-odd effect. This is because the bremsstrahlung- and neutron-induced fissions of ^{232}Th and ^{238}U exhibit maximum even-odd effect at excitation energies near the fission barrier. Similarly, around

[a] e-mail: naikhbarc@yahoo.com

the GDR region the bremsstrahlung- and neutron-induced fissions of ^{232}Th and ^{238}U exhibit significant fission and reaction cross-sections.

Data on fission product yields in the low-energy neutron-induced fission of actinides are available in various compilations [16–20]. Sufficient data on fission product yields in the reactor neutron- [21,22] and mono-energetic neutron-induced [23–48] fissions of ^{238}U are also available in the literature. On the other hand, yields of fission fragments in the excitation energy range of the GDR region due to electromagnetic fission in inverse kinematics [49–51] are available for neutron-deficient lighter-mass actinides (*e.g.*, $^{231-234}$U). Similarly, data on fission product yields in the bremsstrahlung-induced fission of ^{234,235,238}U are also available in the literature [52–72] over a broad energy range.

From the above-mentioned data, it can be seen that in the photon- and neutron-induced fissions of ^{238}U the yields of fission products around mass numbers 133–135, 138–140 and 143–145 and their complementary products are higher than the other fission products. This is due to the effect of the nuclear structure such as the even-odd effect [73]. Besides this, higher yields of fission products around mass number 133–135 and 143–145 is also explainable from the point of view of the standard I and standard II asymmetric fission modes as mentioned by Brossa *et al.* [74], which arise due to the shell effect [75]. The role of the nuclear structure effect is clear around the excitation energy above second saddle. It has been shown by Pomme *et al.* [68] that in the bremsstrahlung-induced fission of ^{238}U, the even-odd effect remains constant up to excitation the energy of 2.2 MeV above the second barrier and thereafter it decreases. Thus it is interesting to examine the effect of the nuclear structure with the increase of the excitation energy beyond 2.2 MeV above second barrier, *i.e.* at the bremsstrahlung energy above 9.5 MeV. In our earlier work at the end point bremsstrahlung energy of 10 MeV [72] the nuclear structure effect was observed. Thus it is worthy to investigate the effect of the nuclear structure above 10 MeV, *i.e.* around the giant dipole resonance (GDR) region, where the fission cross-section is significantly high. In view of this, in the present work the yields of various fission products in the 11.5, 13.4, 15.0 and 17.3 MeV bremsstrahlung-induced fission of ^{238}U have been determined by using the off-line gamma-ray spectrometric technique at the electron linac, SAPHIR at CEA, Saclay, France.

2 Experimental details

The experiment was performed by using a bremsstrahlung beam with end point energies of 11.5, 13.4, 15.0 and 17.3 MeV, produced from electron linac, SAPHIR at CEA, Saclay, France. The bremsstrahlung beam was produced by impinging a pulsed electron beam on a light water-cooled cylindrical tungsten target of 5 cm diameter and 5 mm thickness.

High-purity natural uranium metal rod of diameter 2.74 mm and length 5 mm weighing 5.6 g was mounted inside a pneumatic rabbit holder. It was irradiated for 30 minutes with the bremsstrahlung radiation using the pneumatic carrier facility. Within few seconds, the pneumatic rabbit allows us to carry the sample from the irradiation room to the front of the detector. Different irradiations were taken for end point energies of 11.5, 13.4, 15.0 and 17.3 MeV, respectively. During the irradiation, the electron linac was operated with a pulse repetition rate of 25 Hz and a pulse width of 2.5 μs. The peak current during irradiation was 100 mA with an average current of 6 μA. The electron beam current was very stable during the irradiation time of 30 minutes. Thus it produced constant photon flux throughout the irradiation. After the irradiation, the sample along with its holder was pneumatically taken out and fixed at a certain distance from the HPGe detector for gamma-ray counting. The γ-rays activities of the fission products were measured by using the ORTEC 40% HPGe detector coupled to a PC based 8K channel analyzer. The resolution of the detector system was 2.0 keV full width at half maximum (FWHM) at the 1332.0 keV γ-line of ^{60}Co. In order to minimize the dead time and coincidence summing effect, an appropriate distance between the sample and the detector was chosen for each measurement. The dead time of the detector system during counting was always kept less than 10%. The γ-ray counting of the sample was done in live time mode and was followed as a function of time. Measurements of the irradiated sample were done for several times with increasing counting time to follow the decay and to have a good counting statistics for the photo-peak of the γ-lines of different fission products. Typical γ-ray spectra of the fission products from the irradiated U sample taken after 15 s and 32 min are shown in figs. 1 and 2, respectively.

3 Calculation and results

3.1 Calculation of the excitation energy

In the present experiment, we have measured yields of fission products in the 11.5, 13.4, 15.0 and 17.3 MeV bremsstrahlung-induced fission of ^{238}U. For the fissioning nuclei, the average excitation energy ($E^*(Ee)$) corresponding to the end point bremsstrahlung energies of 11.5–17.3 MeV was obtained as done in our earlier work [72] based on the relation [62]

$$E^*(E_e) = \frac{\int_0^{E_e} EN(E_e,E)\sigma_F(E)\mathrm{d}E}{\int_0^{E_e} N(E_e,E)\sigma_F(E)\mathrm{d}E}\,, \qquad (1)$$

where $N(Ee,E)$ is the number of photons at energy E for electron energy Ee, $\sigma_F(E)$ is the photo-fission cross-section of ^{238}U as a function of the photon energy (E).

The bremsstrahlung spectrum $N(Ee,E)$ corresponding to an incident electron energy (Ee) was calculated using EGS4 computer code [76]. The photo-fission cross-sections of ^{238}U in the sub-barrier region [77] and the energy range 5–18.3 MeV [78,79] are available in the literature. In eq. (1), the value of $N(Ee,E)$ from the EGS4

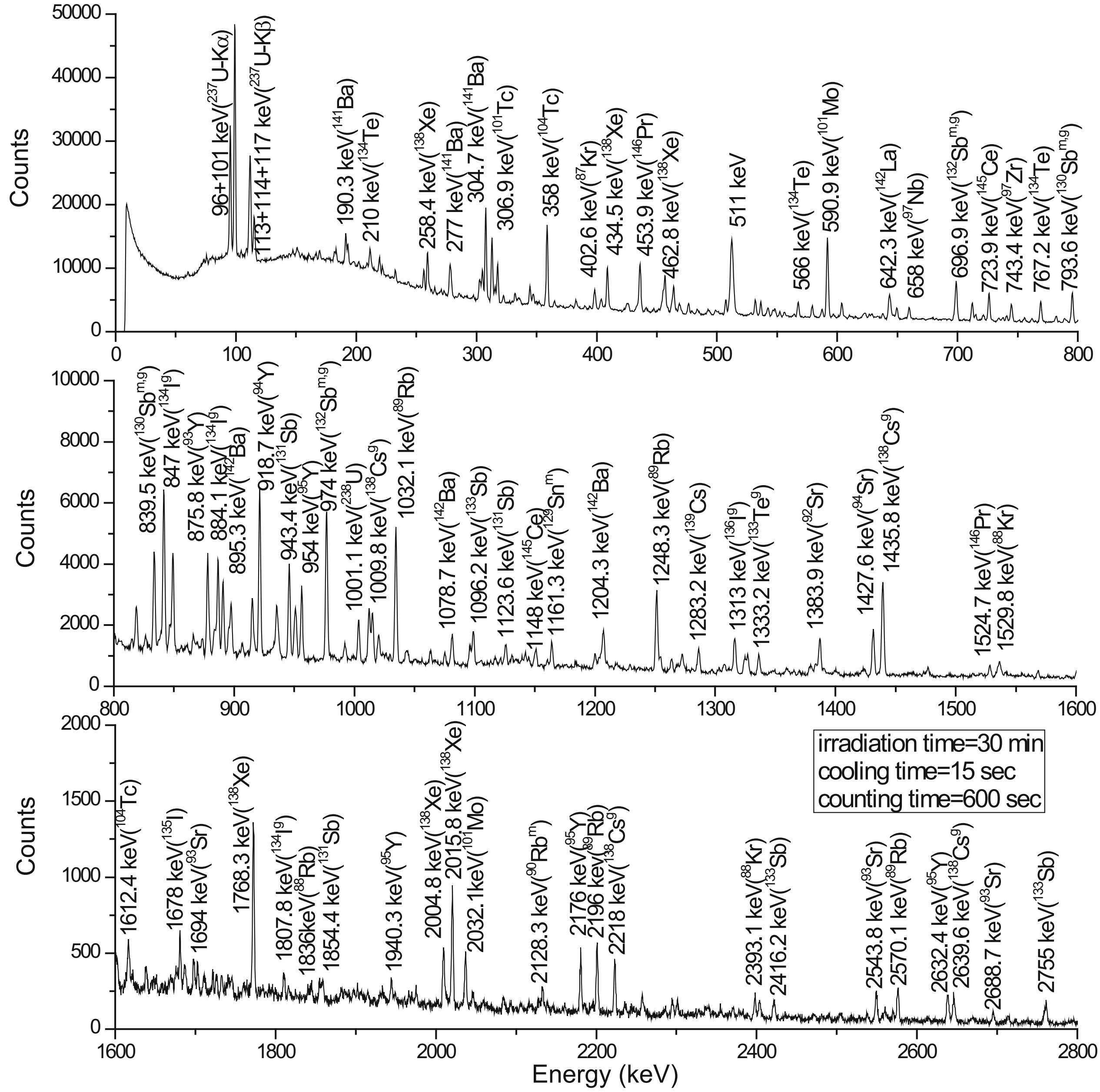

Fig. 1. Typical γ-ray spectra of various fission products after cooling time of 15 s and counting time of 600 s

code [76] and $\sigma_F(E)$ from the experiment [78] were used to calculate the average excitation energy. For the end point bremsstrahlung energies of 11.5, 13.4, 15.0 and 17.3 MeV, the corresponding average excitation energies were found to be 9.09, 10.38, 11.6 and 12.71 MeV, respectively.

3.2 Calculation of yields of fission products from the photo-peak areas

From the gross photo-peak area, the number of detected γ-rays ($A_{\rm obs}$) for different γ-rays of the nuclides of interest was obtained by subtracting the linear Compton background. The $A_{\rm obs}$ of each individual fission product is related to their cumulative yields through the standard decay equation [72],

$$A_{obs}\left(\frac{CL}{LT}\right)=\frac{n\sigma_F(E)\Phi I_\gamma Y(1-e^{-\lambda t})e^{-\lambda T}(1-e^{-\lambda t})}{\lambda}, \quad (2)$$

where Y is the cumulative yield of the fission product, n is the number of target atoms and $\sigma_F(E)$ is the photo-fission cross-section of the target nuclei for the bremsstrahlung spectrum with end point energies of 11.5, 13.4, 15.0 and 17.3 MeV, respectively. $\Phi=\int_{Eb}^{Ee}\varphi \mathrm{d}E$ is the bremsstrahlung flux with photon flux φ from the fission barrier (E_b) to the end point energy (E_e). ε and I_γ are the detection efficiency and branching intensity for the γ-ray

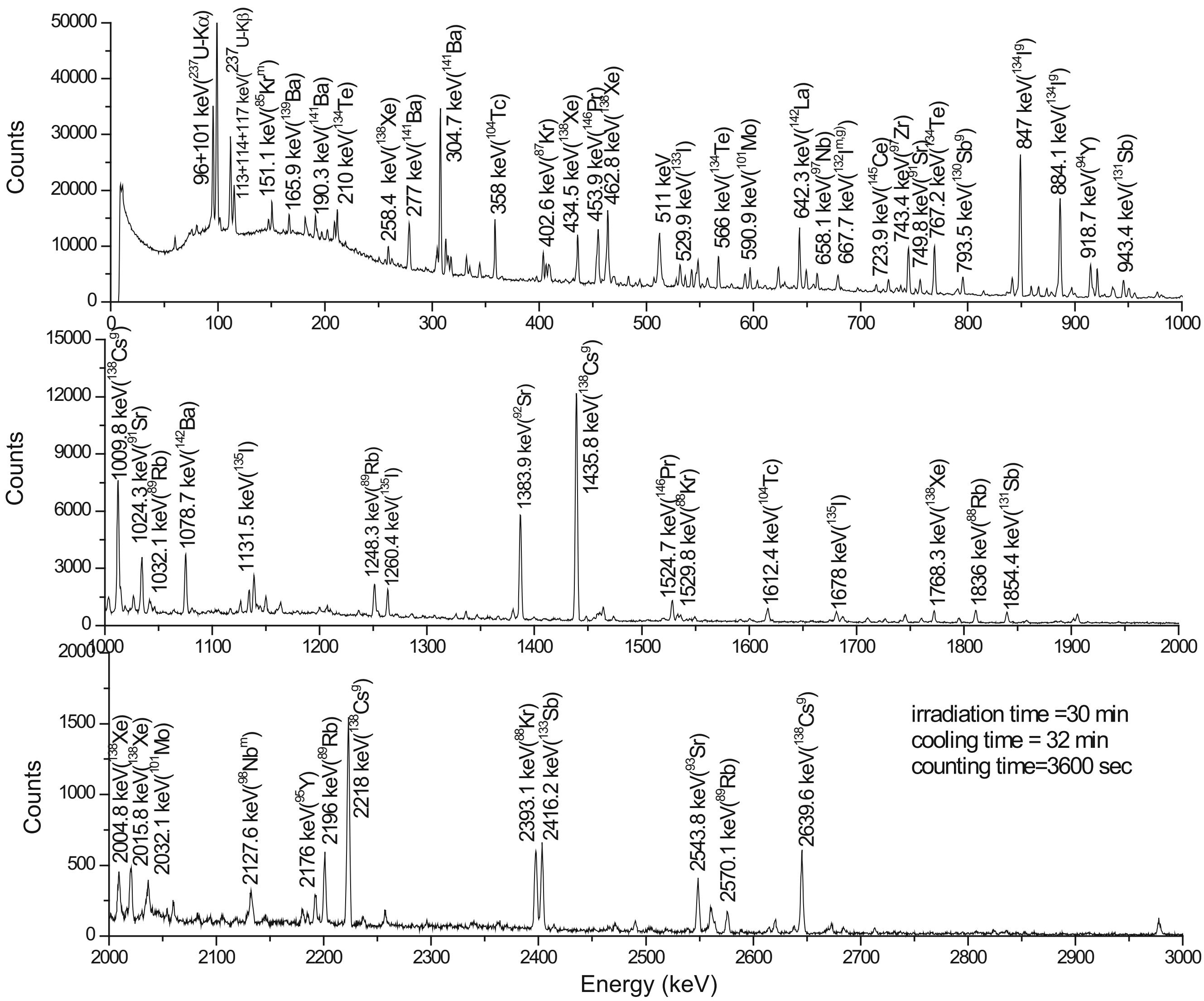

Fig. 2. Typical γ-ray spectra of various fission products after cooling time of 32 min and counting time of 3600 s.

of the fission product nuclide of interest; λ is the decay constant related to the half-life of the fission product of interest ($\lambda = \ln 2/T_{1/2}$); t and T are the irradiation and cooling times, whereas CL and LT are the clock time and live time of counting, respectively.

The nuclear spectroscopic data, such as the γ-ray energy, branching intensity and half-life of the fission products were taken from refs. [80,81]. The rate of fission ($n\sigma_F(E)\Phi$) was first obtained from the photo-peak activity (A_{obs}) of the γ-lines for the fission product ^{135}I and by using the cumulative yield as 1 in eq. (2). This was done because the precursor of ^{135}I is ^{135}Te, which is very short-lived ($T_{1/2} = 19.0$ s). Then the $n\sigma_F(E)\Phi$ term was used in the same eq. (2) to calculate the cumulative yields (Y_R) of other fission products relative to fission rate monitor ^{135}I. For some of the fission product like ^{112}Ag, its precursor, ^{112}Pd, is long-lived ($T_{1/2} = 21.03$ h). Thus there is an equilibrium between ^{112}Pd and ^{112}Ag. The cumulative yield of ^{112}Pd and independent yield of ^{112}Ag is possible to obtain from the decay growth equation by using the activity of the 617 keV γ-line. Otherwise the half-life of ^{112}Pd and the activity of 617 keV γ-line can be used to determine the cumulative yield of ^{112}Ag, which has been done in the present work. Similar is the problem for the fission products ^{105}Ru – ^{105}Rh, ^{131}Sb – ^{131}I, ^{134}Te – ^{134}I, ^{141}Ba – ^{141}Ce, ^{142}Ba – ^{142}La and ^{146}Ce – ^{146}Pr. As, for example, in the case of ^{134}Te – ^{134}I, the cumulative yield of ^{134}Te has been determined from the activities of 566 and 767 keV γ-lines. To determine the cumulative yields of ^{134}I, it is necessary to use the decay growth equation and the activity of the 847 and 884 keV γ-lines. Otherwise it is necessary to wait up to the six half-lives decay of ^{134}Te and then eq. (2) can be used to determine the cumulative yield of ^{134}I from the activities of 847 and 884 keV γ-lines. In the present work, the latter method was followed to determine the cumulative yield of ^{134}I. In the case of ^{146}Pr also, its cumulative yield has been determined from eq. (2) by using the activity of 454 keV γ-line of the spectra after six half-lives decay of ^{146}Ce. Similar is the case for the cumulative yields of the fission products ^{105}Rh, ^{131}I, ^{141}Ce and ^{142}La, respectively.

From the relative cumulative yields (Y_R) of the fission products, their relative mass chain yields (Y_A) were calculated by using Wahl's prescription of charge distribution [20]. According to this, the fractional cumulative yield (Y_{FCY}) of a fission product in an isobaric mass chain is given as

$$FCY = \frac{EOF^{a(Z)}}{\sqrt{2\pi\sigma_Z^2}} \int_{-\infty}^{Z+0.5} \exp\left[-\frac{(Z-Z_P)^2}{2\sigma_Z^2}\right] \mathrm{d}Z, \quad (3)$$

$$Y_A = \frac{Y_R}{Y_{FCY}}, \quad (4)$$

where Z_P is the most probable charge and σ_Z is the width parameter of an isobaric yield distribution. $EOF^{a(Z)}$ is the even-odd effect with $a(Z) = +1$ for even-Z nuclides and -1 for odd-Z nuclides.

For the calculation of Y_{FCY} value of a fission product and mass chain yield of an isobaric mass chain, it is necessary to have knowledge of Z_P, σ_Z and $EOF^{a(Z)}$. In the bremsstrahlung-induced fission of ^{238}U, the Z_P, σ_Z and $EOF^{a(Z)}$ values can be obtained from the fission yield data of ref. [68]. Similarly, systematic data on the charge distribution in the reactor neutron-induced (average $En = 1.9\,\text{MeV}$) fission of different actinides are also available in ref. [73]. It can be seen from ref. [73] that the average width parameter ($\langle\sigma_Z\rangle$) in the reactor neutron-induced fission of ^{238}U is 0.55 ± 0.07. On the other hand, in the proton-induced fission of ^{238}U at medium excitation energy [82], the value of $\langle\sigma_Z\rangle$ is found to be 0.72 ± 0.06. In view of this, the average width parameter ($\langle\sigma_Z\rangle$) value of 0.6 from refs. [68,73,82] was used in the 11.5–17.3 MeV bremsstrahlung-induced fission of ^{238}U. The mass dependence of the even-odd factor on σ_Z was not considered, which may give rise to an error of 3–5% in the FCY value. The Z_P values of individual mass chain (A) for the above fission systems were calculated using the prescription of Umezawa *et al.* [82] given below,

$$Z_P = \eta Z_P \pm \Delta Z_P,\ \eta Z_F = Z_{UCD} = \left(\frac{Z_F}{A_F}\right)(A + v_{\text{post}}), \quad (5a)$$

$$\eta = \frac{A + v_{\text{post}}}{A_C - v_{\text{pre}}}, \quad A_F = A_C - v_{\text{pre}}, \quad (5b)$$

where Z_C and A_C are the charge and mass of the compound nucleus, Z_F and A_F are the charge and mass of the fission system and Z_{UCD} is the most probable charge based on the unchanged charge-density distribution as suggested by Sugarman and Turkevich [83]. A is the mass of the fission product, whereas v_{pre} and v_{post} are pre- and post-fission neutrons. ΔZ_P ($Z_P - Z_{UCD}$) is the charge polarization parameter. The + and – signs for the ΔZ_P value are applicable to light and heavy fragments, respectively.

The pre- (v_{pre}) and post-scission (v_{post}) neutrons in the medium energy fission of actinides can be calculated based on the prescription of Strecker *et al.* [84] or Umezawa *et al.* [82]. The saw tooth nature of post-fission neutron emission trend as a function of fission fragment mass is possible to obtain by Strecker *et al.* [84] but not by Umezawa *et al.* [82]. However, in the present work, the prescription of Umezawa *et al.* [82] was used. This is because the other parameters of charge distribution systematics were taken from the same ref. [82]. Accordingly, the pre- (v_{pre}) and post-scission (v_{post}) neutrons calculated using the relation given below [82],

$$v_{\text{pre}} = \frac{E^*}{7.5 \pm 0.5} + \frac{Z_c^2}{2A_c} - (19.0 \pm 0.5), \quad (6a)$$

$$v_{\text{post}} = 1.0 \quad \text{for} \quad A > 88,$$
$$v_{\text{post}} = 1.0 + 0.1(A - 88) \quad \text{for} \quad 78 < 88,$$
$$v_{\text{post}} = 0 \quad \text{for} \quad A < 78, \quad (6b)$$

where E^* is the excitation energy of the compound nucleus. For the end point bremsstrahlung energies of 11.5, 13.4, 15.0 and 17.3 MeV, the excitation energies of the compound nucleus are 9.09, 10.38, 11.6 and 12.71 MeV, respectively. The excitation energies were used in eq. (6a) to calculate the v_{pre} values at three different neutron energies. The of v_{pre} and v_{post} obtained based on eqs. (6a) and (6b) are used in eqs. (5a) and (5b) to obtain the value of Z_{UCD} as a function of mass number for the different fission product. The ΔZ_P value was then calculated by using the following relation [82]:

$$\Delta Z_P = 0 \quad \text{for} \quad I\eta - 0.5I < 0.4, \quad (7a)$$

$$\Delta Z_P = \left(\frac{20}{3}\right)(I\eta - 0.5I - 0.04) \text{ for } 0.04 < I\eta$$
$$-0.5I < 0.085. \quad (7b)$$

The ΔZ_P values obtained in the above way for different mass chains were used in eq. (5a) to obtain the Z_P value. Then the Z_P and the σ_Z values of 0.6 were used in eq. (3) to calculate the Y_{FCY} value of the individual fission products. The relative cumulative yields (Y_R) of the individual fission products and their Y_{FCY} values were used in eq. (4) to obtain their relative mass chains yields (Y_A). The relative mass chain yields of the fission products obtained were then normalized to a total yield of 200% to calculate the absolute mass chain yields. The absolute cumulative yields (Y) of the fission products in the 11.5, 13.4, 15.0 and 17.3 MeV bremsstrahlung-induced fission of ^{238}U were then obtained by using the mass yield data and Y_{FCY} values. The absolute cumulative yields (Y) of the individual fission products and their mass chain yields in the 11.5–17.3 MeV bremsstrahlung-induced fission of ^{238}U along with the nuclear spectroscopic data from refs. [80, 81] are given in tables 1–4. The uncertainty shown in the measured cumulative yield of individual fission products in tables 1–4 is the fluctuation of the mean value from several measurements. The overall uncertainty represents contributions from both random and systematic errors.

Table 1. Nuclear spectroscopic data and yields of fission products in the 11.472 MeV photon-induced fission of ^{238}U.

Nuclide	Half-life	γ-ray energy (keV)	γ-ray abundance (%)	Y_R (%)$^{(a)}$	Y_A (%)$^{(b)}$
^{84}Br	31.8 min	881.6	43.0	0.665 ± 0.066	0.665 ± 0.066
		1616.2	6.2	0.723 ± 0.078	0.723 ± 0.078
^{85}Kr^{m}	4.48 h	151.2	75.0	0.929 ± 0.062	0.929 ± 0.062
		304.9	14.0	0.896 ± 0.056	0.896 ± 0.056
^{87}Kr	76.3 min	402.6	49.6	1.652 ± 0.177	1.658 ± 0.178
^{88}Kr	2.84 h	196.3	25.9	2.331 ± 0.188	2.347 ± 0.189
^{89}Rb	15.2 min	1032.1	58.0	3.321 ± 0.201	3.321 ± 0.201
		1248.3	42.6	2.931 ± 0.228	2.931 ± 0.228
^{91}Sr	9.63 h	749.8	23.6	3.727 ± 0.245	3.727 ± 0.245
		1024.3	33.0	3.966 ± 0.301	3.966 ± 0.301
^{92}Sr	2.71 h	1384.9	90.0	4.325 ± 0.111	4.333 ± 0.111
^{93}Y	10.18 h	266.9	7.3	3.973 ± 0.239	3.973 ± 0.239
^{94}Y	18.7 m	918.7	56.0	4.033 ± 0.150	4.033 ± 0.150
^{95}Zr	64.02 d	756.7	54.0	4.962 ± 0.195	4.962 ± 0.195
		724.3	44.2	5.154 ± 0.192	5.154 ± 0.192
^{97}Zr	16.91 h	743.4	93.0	6.145 ± 0.305	6.158 ± 0.306
^{99}Mo	65.94 h	140.5	89.4	5.628 ± 0.178	5.639 ± 0.178
		739.5	12.13	5.611 ± 0.244	5.623 ± 0.245
^{101}Mo	14.61 min	590.1	16.4	7.102 ± 0.188	7.131 ± 0.189
^{103}Ru	39.26 d	497.1	90.0	4.940 ± 0.161	4.940 ± 0.161
^{104}Tc	18.3 min	358.0	89.0	3.276 ± 0.312	3.276 ± 0.312
^{105}Ru	4.44 h	724.4	47.0	2.614 ± 0.116	
^{105}Rh	35.36 h	319.1	19.2	2.627 ± 0.102	2.627 ± 0.102
^{107}Rh	21.7 min	302.8	66.0	1.079 ± 0.028	1.079 ± 0.028
^{112}Ag	3.13 h	617.5	43.0	0.112 ± 0.022	0.112 ± 0.022
^{113}Ag	5.37 h	298.6	10.0	0.107 ± 0.017	0.107 ± 0.017
^{115}Cd^{g}	53.46 h	336.2	45.9	0.079 ± 0.022	0.079 ± 0.022
^{115}Cd^{total}				$0.095 \pm 0.022^{(c)}$	$0.095 \pm 0.022^{(c)}$
^{117}Cd^{m}	3.36 h	1066.0	23.1	$.0072 \pm .0005$	
		1097.3	26.0	$.0074 \pm .0006$	
^{117}Cd^{g}	2.49 h	273.4	28.0	$.0668 \pm .0056$	
^{117}Cd^{total}				$.0741 \pm .0061$	$.0741 \pm .0061$
^{127}Sb	3.85 d	687.0	37.0	0.344 ± 0.089	0.344 ± 0.089
^{128}Sn	59.07 min	482.3	59.0	0.623 ± 0.049	0.645 ± 0.050
^{129}Sb	4.32 h	812.4	43.0	1.163 ± 0.078	1.163 ± 0.078
^{131}Sb	23.03 min	943.4	47.0	3.805 ± 0.233	
^{131}I	8.02 d	364.5	81.7	4.194 ± 0.267	4.194 ± 0.267
^{132}Te	3.2 d	228.1	88.0	5.307 ± 0.322	5.318 ± 0.323
^{133}I	20.8 h	529.9	87.0	7.688 ± 0.217	7.688 ± 0.217
^{134}Te	41.8 min	566.0	18.0	7.243 ± 0.289	7.815 ± 0.312
		767.2	29.5	7.683 ± 0.267	8.288 ± 0.289
^{134}I	52.5 min	847.0	95.4	8.067 ± 0.367	8.067 ± 0.367
		884.1	65.0	8.245 ± 0.306	8.245 ± 0.306
^{135}I$^{(d)}$	6.57 h	1131.5	22.7	5.679 ± 0.260	5.713 ± 0.261
		1260.4	28.9	5.563 ± 0.055	5.996 ± 0.056
^{137}Xe	3.7 min	455.5	31.0	6.585 ± 0.167	6.585 ± 0.167
^{138}Cs^{g}	33.41 min	1435.8	76.3	7.065 ± 0.362	7.079 ± 0.362
		1009.8	29.8	6.825 ± 0.283	6.839 ± 0.283
		462.8	30.7	6.942 ± 0.288	6.956 ± 0.289
^{139}Ba	83.03 min	165.8	23.7	6.565 ± 0.362	6.565 ± 0.362
^{140}Ba	12.75 d	537.3	24.4	5.396 ± 0.217	5.396 ± 0.217
^{141}Ba	18.27 min	190.3	46.0	3.848 ± 0.161	
		304.7	35.4	4.115 ± 0.178	

Table 1. Continued.

Nuclide	Half-life	γ-ray energy (keV)	γ-ray abundance (%)	Y_{R} (%)	Y_{A} (%)
^{141}Ce	32.5 d	145.4	48.0	4.539 ± 0.350	4.539 ± 0.350
^{142}Ba	10.6 min	255.3	20.5	4.689 ± 0.134	
^{142}La	91.1 min	641.3	47.0	4.751 ± 0.217	4.751 ± 0.217
^{143}Ce	33.03 h	293.3	42.8	5.035 ± 0.250	5.035 ± 0.250
^{144}Ce	284.89 d	133.5	11.09	4.863 ± 0.206	4.863 ± 0.206
^{146}Ce	13.52 min	316.7	56.0	2.837 ± 0.095	
		218.2	20.6	2.742 ± 0.117	
^{146}Pr	24.15 min	453.9	48.0	3.087 ± 0.189	3.087 ± 0.189
		1524.7	15.6	3.126 ± 0.195	3.126 ± 0.195
^{147}Nd	10.98 d	531.0	13.1	2.064 ± 0.078	2.064 ± 0.078
^{149}Nd	1.728 h	211.3	25.9	1.240 ± 0.078	
		270.2	10.6	1.202 ± 0.061	
^{149}Pm	53.08 h	286.0	3.1	1.285 ± 0.078	1.285 ± 0.078
^{151}Pm	53.08 h	340.8	23.0	0.745 ± 0.039	0.745 ± 0.039
^{153}Sm	46.28 h	103.2	30.0	0.295 ± 0.011	0.295 ± 0.011

(a) Y_R – Cumulative yields.
(b) Y_A – Mass yields.
(c) The yields of ^{115}Cd$^{\mathrm{total}}$ are based on the ratio of ^{115}Cd$^{\mathrm{g}}$/^{115}Cd$^{\mathrm{m}}$ = 6 from ref. [38].
(d) ^{135}I – Fission rate monitor.

Table 2. Nuclear spectroscopic data and yields of fission products in the 13.390 MeV photon-induced fission of ^{238}U.

Nuclide	Half-life	γ-ray Energy (keV)	γ-ray abundance (%)	Y_R (%)	Y_A (%)
^{84}Br	31.8 min	881.6	43.0	0.793 ± 0.051	0.793 ± 0.051
		1616.2	6.2	0.860 ± 0.039	0.860 ± 0.039
^{85}Kr$^{\mathrm{m}}$	4.48 h	151.2	75.0	0.989 ± 0.062	0.989 ± 0.062
		304.9	14.0	0.977 ± 0.051	0.977 ± 0.051
^{87}Kr	76.3 min	402.6	49.6	1.692 ± 0.101	1.692 ± 0.101
^{88}Kr	2.84 h	196.3	25.9	2.400 ± 0.213	2.411 ± 0.214
^{89}Rb	15.2 min	1032.1	58.0	2.928 ± 0.180	2.928 ± 0.180
		1248.3	42.6	3.119 ± 0.202	3.119 ± 0.202
^{91}Sr	9.63 h	749.8	23.6	3.749 ± 0.236	3.749 ± 0.236
		1024.3	33.0	3.665 ± 0.146	3.665 ± 0.146
^{92}Sr	2.71 h	1384.9	90.0	4.395 ± 0.252	4.395 ± 0.252
^{93}Y	10.18 h	266.9	7.3	3.861 ± 0.129	3.861 ± 0.129
^{94}Y	18.7 m	918.7	56.0	4.016 ± 0.146	4.016 ± 0.146
^{95}Zr	64.02 d	756.7	54.0	4.813 ± 0.275	4.813 ± 0.275
		724.3	44.2	4.954 ± 0.197	4.954 ± 0.197
^{97}Zr	16.91 h	743.4	93.0	5.822 ± 0.258	5.834 ± 0.259
^{99}Mo	65.94 h	140.5	89.4	5.637 ± 0.174	5.648 ± 0.174
		739.5	12.13	5.733 ± 0.258	5.744 ± 0.259
^{101}Mo	14.61 min	590.1	16.4	7.919 ± 0.319	7.959 ± 0.321
^{103}Ru	39.26 d	497.1	90.0	5.407 ± 0.271	5.407 ± 0.271
^{104}Tc	18.3 min	358.0	89.0	3.710 ± 0.259	3.710 ± 0.259
^{105}Ru	4.44 h	724.4	47.0	2.490 ± 0.096	
^{105}Rh	35.36 h	319.1	19.2	2.698 ± 0.180	2.698 ± 0.180
^{107}Rh	21.7 min	302.8	66.0	1.147 ± 0.152	1.147 ± 0.152
^{112}Ag	3.13 h	617.5	43.0	0.188 ± 0.045	0.188 ± 0.045
^{113}Ag	5.37 h	298.6	10.0	0.179 ± 0.051	0.179 ± 0.051
^{115}Cd$^{\mathrm{g}}$	53.46 h	336.2	45.9	0.141 ± 0.028	0.141 ± 0.028
^{115}Cd$^{\mathrm{total}}$				$0.165 \pm 0.028^{*}$	$0.165 \pm 0.028^{*}$
^{117}Cd$^{\mathrm{m}}$	3.36 h	1066.0	23.1	$.0191 \pm .0045$	
		1097.3	26.0	$.0189 \pm .0055$	
^{117}Cd$^{\mathrm{g}}$	2.49 h	273.4	28.0	$.1349 \pm .0225$	
^{117}Cd$^{\mathrm{total}}$				$.1540 \pm .0231$	$.1540 \pm .0231$
^{127}Sb	3.85 d	687.0	37.0	0.331 ± 0.022	0.331 ± 0.022
^{128}Sn	59.07 min	482.3	59.0	0.680 ± 0.072	0.680 ± 0.073

Table 2. Continued.

Nuclide	Half-life	γ-ray Energy (keV)	γ-ray abundance (%)	Y_R (%)	Y_A (%)
^{129}Sb	4.32 h	812.4	43.0	1.338 ± 0.079	1.338 ± 0.079
^{131}Sb	23.03 min	943.4	47.0	3.771 ± 0.107	
^{131}I	8.02 d	364.5	81.7	3.878 ± 0.112	3.878 ± 0.112
^{132}Te	3.2 d	228.1	88.0	5.351 ± 0.123	5.362 ± 0.124
^{133}I	20.8 h	529.9	87.0	7.425 ± 0.271	7.442 ± 0.272
^{134}Te	41.8 min	566.0	18.0	7.577 ± 0.289	8.296 ± 0.317
		767.2	29.5	7.740 ± 0.248	8.476 ± 0.272
^{134}I	52.5 min	847.0	95.4	8.437 ± 0.372	8.437 ± 0.372
		884.1	65.0	8.303 ± 0.311	8.303 ± 0.311
^{135}I	6.57 h	1131.5	22.7	5.671 ± 0.073	5.716 ± 0.073
		1260.4	28.9	5.621 ± 0.056	5.621 ± 0.056
^{137}Xe	3.7 min	455.5	31.0	6.525 ± 0.179	6.525 ± 0.179
^{138}Cs^{g}	33.41 min	1435.8	76.3	7.088 ± 0.281	7.102 ± 0.282
		1009.8	29.8	6.762 ± 0.258	6.776 ± 0.259
		462.8	30.7	6.852 ± 0.196	6.866 ± 0.197
^{139}Ba	83.03 min	165.8	23.7	5.941 ± 0.259	5.941 ± 0.259
^{140}Ba	12.75 d	537.3	24.4	4.828 ± 0.236	4.828 ± 0.236
^{141}Ba	18.27 min	190.3	46.0	3.912 ± 0.197	
		304.7	35.4	3.951 ± 0.141	
^{141}Ce	32.5 d	145.4	48.0	4.266 ± 0.259	4.266 ± 0.259
^{142}Ba	10.6 min	255.3	20.5	4.764 ± 0.202	
^{142}La	91.1 min	641.3	47.0	4.907 ± 0.287	4.907 ± 0.287
^{143}Ce	33.03 h	293.3	42.8	4.940 ± 0.146	4.940 ± 0.146
^{144}Ce	284.89 d	133.5	11.09	4.759 ± 0.108	4.759 ± 0.108
^{146}Ce	13.52 min	316.7	56.0	3.361 ± 0.067	
		218.2	20.6	3.216 ± 0.146	
^{146}Pr	24.15 min	453.9	48.0	3.389 ± 0.236	3.389 ± 0.236
		1524.7	15.6	3.592 ± 0.107	3.592 ± 0.107
^{147}Nd	10.98 d	531.0	13.1	2.361 ± 0.185	2.361 ± 0.185
^{149}Nd	1.728 h	211.3	25.9	1.225 ± 0.067	
		270.2	10.6	1.214 ± 0.062	
^{149}Pm	53.08 h	286.0	3.1	1.349 ± 0.084	1.349 ± 0.084
^{151}Pm	53.08 h	340.8	23.0	0.776 ± 0.039	0.776 ± 0.039
^{153}Sm	46.28 h	103.2	30.0	0.315 ± 0.011	0.315 ± 0.011

(a) Y_R – Cumulative yields.
(b) Y_A – Mass yields.
(c) The yields of ^{115}Cd$^{\text{total}}$ is based on the ratio of ^{115}Cd^{g}/^{115}Cd^{m} = 6 from ref. [38]
(d) ^{135}I – Fission rate monitor.

The random error in the observed activity is due to counting statistics and is estimated to be 10–15%, which can be determined by accumulating the data for the optimum period of time, depending on the half-life of the nuclide of interest. On the other hand, the systematic errors are due to the uncertainties in the irradiation time (0.5%), detector efficiency calibration ($\sim$ 3%), half-life of nuclides of the fission products ($\sim$ 1%) and the γ-ray abundance ($\sim$ 2%), which are the largest variation in the literature [80,81]. Thus, the overall systematic error is about 3.8%. An upper limit of error of 10.7–15.5% was determined at for the fission product yields based on 10–15% random error and a 3.8% systematic error.

4 Discussion

The yields of various fission products shown in tables 1–4 in the 13.4 and 17.3 MeV bremsstrahlung-induced fission of ^{238}U were determined for the first time. On the other hand, the fission yields data in ^{238}U(γ, f) at end point bremsstrahlung energies of 11.5 and 15 MeV are the redetermined values but are in close agreement with the similar data of Pomme *et al.* [69] at 11.13 MeV and Jacobs *et al.* [64] at 15 MeV. The mass chain yields of various fission products in the 11.5–17.3 MeV bremsstrahlung-induced fission of ^{238}U from present work are plotted in fig. 3. Similarly, the mass chain yields data in the 3.9,

Table 3. Nuclear spectroscopic data and yields of fission products in the 14.987 MeV photon-induced fission of ^{238}U.

Nuclide	Half-life	γ-ray Energy (keV)	γ-ray abundance (%)	Y_R (%)	Y_A (%)
^{84}Br	31.8 min	881.6	43.0	0.875 ± 0.061	0.875 ± 0.061
		1616.2	6.2	0.925 ± 0.052	0.925 ± 0.052
^{85}Kr^{m}	4.48 h	151.2	75.0	1.098 ± 0.045	1.098 ± 0.045
		304.9	14.0	1.148 ± 0.051	1.148 ± 0.051
^{87}Kr	76.3 min	402.6	49.6	1.855 ± 0.295	1.855 ± 0.295
^{88}Kr	2.84 h	196.3	25.9	2.579 ± 0.189	2.585 ± 0.189
^{89}Rb	15.2 min	1032.1	58.0	3.075 ± 0.128	3.075 ± 0.128
		1248.3	42.6	3.170 ± 0.184	3.170 ± 0.184
^{91}Sr	9.63 h	749.8	23.6	3.621 ± 0.139	3.621 ± 0.139
		1024.3	33.0	3.749 ± 0.095	3.749 ± 0.095
^{92}Sr	2.71 h	1384.9	90.0	4.261 ± 0.128	4.273 ± 0.128
^{93}Y	10.18 h	266.9	7.3	3.998 ± 0.212	3.998 ± 0.212
^{94}Y	18.7 m	918.7	56.0	4.473 ± 0.251	4.473 ± 0.251
^{95}Zr	64.02 d	756.7	54.0	5.268 ± 0.239	5.268 ± 0.239
		724.3	44.2	5.172 ± 0.279	5.172 ± 0.279
^{97}Zr	16.91 h	743.4	93.0	5.779 ± 0.172	5.810 ± 0.173
^{99}Mo	65.94 h	140.5	89.4	5.137 ± 0.223	5.149 ± 0.223
		739.5	12.13	5.091 ± 0.067	5.091 ± 0.067
^{101}Mo	14.61 min	590.1	16.4	7.125 ± 0.301	7.139 ± 0.302
^{103}Ru	39.26 d	497.1	90.0	4.947 ± 0.245	4.947 ± 0.245
^{104}Tc	18.3 min	358.0	89.0	3.654 ± 0.284	3.654 ± 0.284
^{105}Ru	4.44 h	724.4	47.0	2.546 ± 0.061	
^{105}Rh	35.36 h	319.1	19.2	2.579 ± 0.051	2.579 ± 0.051
^{107}Rh	21.7 min	302.8	66.0	1.164 ± 0.089	1.164 ± 0.089
^{112}Ag	3.13 h	617.5	43.0	0.206 ± 0.022	0.206 ± 0.022
^{113}Ag	5.37 h	298.6	10.0	0.195 ± 0.017	0.195 ± 0.017
^{115}Cd^{g}	53.46 h	336.2	45.9	0.163 ± 0.028	0.163 ± 0.028
^{115}Cd^{total}				$0.190 \pm 0.028^{*}$	$0.190 \pm 0.028^{*}$
^{117}Cd^{m}	3.36 h	1066.0	23.1	$.0256 \pm .0022$	
		1097.3	26.0	$.0267 \pm .0035$	
^{117}Cd^{g}	2.49 h	273.4	28.0	$.1615 \pm .0222$	
^{117}Cd^{total}				$.1877 \pm .0228$	$.1877 \pm .0228$
^{127}Sb	3.85 d	687.0	37.0	0.529 ± 0.028	0.529 ± 0.028
^{128}Sn	59.07 min	482.3	59.0	0.847 ± 0.037	0.867 ± 0.037
^{129}Sb	4.32 h	812.4	43.0	1.348 ± 0.162	1.348 ± 0.162
^{131}Sb	23.03 min	943.4	47.0	4.183 ± 0.184	
^{131}I	8.02 d	364.5	81.7	4.217 ± 0.151	4.217 ± 0.151
^{132}Te	3.2 d	228.1	88.0	5.482 ± 0.139	5.493 ± 0.139
^{133}I	20.8 h	529.9	87.0	6.791 ± 0.334	6.791 ± 0.334
^{134}Te	41.8 min	566.0	18.0	7.247 ± 0.318	7.966 ± 0.324
		767.2	29.5	7.214 ± 0.345	8.149 ± 0.396

5.5, 6.9 and 7.7 MeV neutron-induced fission of ^{238}U from the literature [38] with comparable excitation energies are plotted in fig. 4. It can be seen from figs. 3 and 4 that in the 11.5–17.3 MeV bremsstrahlung- and 3.9–7.7 MeV neutron-induced fission of ^{238}U, the yields of fission products for $A = 133$–134, 138–139 and 143–144 and their complementary products are higher than the other fission products. This indicates the effect of the nuclear structure. A similar effect has also been predicted earlier in the bremsstrahlung-induced fission of ^{238}U at other energies [52–72] as well as in the neutron-induced fission [21–48] of ^{238}U, which supports the present observation. The higher yields of the fission products around the mass number 133–134 and 143–144 and their complementary products can be explained from the point of view of the standard I and standard II asymmetric fission modes mentioned by Brossa *et al.* [74], which arise due to shell effects [75]. Based on standard I asymmetry, the fissioning system is characterized by spherical heavy fragment mass numbers 133–134 due to the spherical $82n$ shell and a deformed complementary light-mass number. Based on standard II asymmetry, the fissioning system is characterized by a deformed heavy-mass fragment near mass numbers of 143–144 due to a deformed $88n$ shell and slightly deformed

Table 3. Continued.

Nuclide	Half-life	γ-ray Energy (keV)	abundance γ-ray (%)	Y_R (%)	Y_A (%)
^{134}I	52.5 min	847.0	95.4	8.184 ± 0.373	8.184 ± 0.373
		884.1	65.0	7.927 ± 0.323	7.927 ± 0.323
^{135}I	6.57 h	1131.5	22.7	5.576 ± 0.184	5.754 ± 0.185
		1260.4	28.9	5.571 ± 0.055	5.649 ± 0.056
^{137}Xe	3.7 min	455.5	31.0	6.743 ± 0.245	6.743 ± 0.245
^{138}Cs^{g}	33.41 min	1435.8	76.3	7.002 ± 0.222	7.016 ± 0.223
		1009.8	29.8	6.802 ± 0.288	6.816 ± 0.289
		462.8	30.7	6.712 ± 0.249	6.725 ± 0.251
^{139}Ba	83.03 min	165.8	23.7	5.871 ± 0.295	5.871 ± 0.295
^{140}Ba	12.75 d	537.3	24.4	5.118 ± 0.229	5.118 ± 0.229
^{141}Ba	18.27 min	190.3	46.0	4.466 ± 0.256	
		304.7	35.4	4.544 ± 0.201	
^{141}Ce	32.5 d	145.4	48.0	4.568 ± 0.239	4.568 ± 0.239
^{142}Ba	10.6 min	255.3	20.5	4.384 ± 0.289	
^{142}La	91.1 min	641.3	47.0	4.688 ± 0.195	4.688 ± 0.195
^{143}Ce	33.03 h	293.3	42.8	4.738 ± 0.139	4.738 ± 0.139
^{144}Ce	284.89 d	133.5	11.09	4.437 ± 0.106	4.437 ± 0.106
^{146}Ce	13.52 min	316.7	56.0	3.158 ± 0.128	
		218.2	20.6	2.874 ± 0.139	
^{146}Pr	24.15 min	453.9	48.0	3.175 ± 0.184	3.175 ± 0.184
		1524.7	15.6	2.986 ± 0.156	2.986 ± 0.156
^{147}Nd	10.98 d	531.0	13.1	2.395 ± 0.162	2.395 ± 0.162
^{149}Nd	1.728 h	211.3	25.9	1.214 ± 0.089	
		270.2	10.6	1.231 ± 0.067	
^{149}Pm	53.08 h	286.0	3.1	1.271 ± 0.028	1.271 ± 0.028
^{151}Pm	53.08 h	340.8	23.0	0.751 ± 0.011	0.751 ± 0.011
^{153}Sm	46.28 h	103.2	30.0	0.318 ± 0.012	0.318 ± 0.012

(a) Y_R – Cumulative yields.
(b) Y_A – Mass yields.
(c) The yields of ^{115}Cd$^{\text{total}}$ is based on the ratio of ^{115}Cd^{g}/^{115}Cd^{m} = 6 from ref. [38].
(d) ^{135}I – Fission rate monitor.

light mass. Thus, the higher yields of fission products for $A = 133$–134 and 143–144 are due to the presence of spherical $82n$ and deformed $88n$ shells, respectively. However, the higher yields of fission products around mass number 138–140 and their complementary products are not possible to explain based on only standard I and standard II asymmetric fission modes [74] unless the even-odd effect is considered. The higher yields of the heavy and light complementary mass fission products are in the interval of five mass and two charge units. This is because the A/Z of the fission products and fissioning system is around 2.5. Thus the difference of two charges makes the oscillation of mass yield in the interval of five mass units. It can be also seen from figs. 3 and 4 that the amplitude of oscillation in the interval of five mass units are comparable in the 11.5–17.3 MeV bremsstrahlung- and 3.9–7.7 MeV neutron-induced fission of ^{238}U. This is in accordance with their even-odd effects [68,73]. However, the even-odd effect is out of phase with shell effect [75] and decreases with excitation energy [68]. The fissioning system ^{238}U* [68] has slightly higher even-odd effect than ^{239}U* [73].

In order to examine the above aspects, the yields of fission products for $A = 133$–134, 138–139 and 143–144 as a function of the excitation energy are shown in table 5 from the present work and literature data [52–72] in ^{238}U(γ, f). Similar data from the literature [23–48] in ^{238}U(n, f) are shown in table 6. The yields of fission products for $A = 134$, 139 and 143 as a function of excitation energy are plotted in fig. 5. It can be seen from fig. 5 that within the uncertainty the yields of fission products around mass 133–134 and their complementary products are slightly higher in ^{238}U(γ, f) than in ^{238}U(n, f). However, the yields of fission products for $A = 139$, 143 and their complementary products are comparable in ^{238}U(γ, f) and ^{238}U(n, f). This is reflected in the lower average heavy mass ($\langle A_{\text{H}} \rangle$ in ^{238}U(γ, f)) compared to ^{238}U(n, f), which shall be discussed later on. These observations cannot be explained based on either the even-odd effect or the standard I and standard II asymmetric modes unless one considers the effect of complementary shell combinations. Around mass number 133–134, the most probable Z is 52, then the fission fragment has spher-

Table 4. Nuclear spectroscopic data and yields of fission products in the 17.278 MeV photon-induced fission of ^{238}U.

Nuclide	Half-life	γ-ray Energy (keV)	γ-ray abundance (%)	Y_R (%)	Y_A (%)
^{84}Br	31.8 min	881.6	43.0	0.886 ± 0.044	0.886 ± 0.044
		1616.2	6.2	0.894 ± 0.038	0.894 ± 0.038
^{85}Kr^{m}	4.48 h	151.2	75.0	1.165 ± 0.088	1.165 ± 0.088
		304.9	14.0	1.126 ± 0.049	1.126 ± 0.049
^{87}Kr	76.3 min	402.6	49.6	2.084 ± 0.241	2.084 ± 0.241
^{88}Kr	2.84 h	196.3	25.9	2.473 ± 0.263	2.478 ± 0.264
^{89}Rb	15.2 min	1032.1	58.0	3.014 ± 0.126	3.014 ± 0.126
		1248.3	42.6	3.129 ± 0.148	3.129 ± 0.148
^{91}Sr	9.63 h	749.8	23.6	3.567 ± 0.088	3.567 ± 0.088
		1024.3	33.0	3.813 ± 0.066	3.813 ± 0.066
^{92}Sr	2.71 h	1384.9	90.0	4.338 ± 0.215	4.343 ± 0.216
^{93}Y	10.18 h	266.9	7.3	3.843 ± 0.104	3.843 ± 0.104
^{94}Y	18.7 m	918.7	56.0	4.245 ± 0.115	4.245 ± 0.115
^{95}Zr	64.02 d	756.7	54.0	5.136 ± 0.159	5.136 ± 0.159
		724.3	44.2	5.436 ± 0.197	5.436 ± 0.197
^{97}Zr	16.91 h	743.4	93.0	6.023 ± 0.197	6.028 ± 0.197
^{99}Mo	65.94 h	140.5	89.4	5.901 ± 0.098	5.901 ± 0.098
		739.5	12.13	5.890 ± 0.234	5.890 ± 0.234
^{101}Mo	14.61 min	590.1	16.4	7.747 ± 0.158	7.762 ± 0.159
^{103}Ru	39.26 d	497.1	90.0	4.781 ± 0.284	4.781 ± 0.284
^{104}Tc	18.3 min	358.0	89.0	3.364 ± 0.213	3.364 ± 0.213
^{105}Ru	4.44 h	724.4	47.0	2.501 ± 0.148	
^{105}Rh	35.36 h	319.1	19.2	2.516 ± 0.181	2.516 ± 0.181
^{107}Rh	21.7 min	302.8	66.0	1.220 ± 0.098	1.220 ± 0.098
^{112}Ag	3.13 h	617.5	43.0	0.299 ± 0.011	0.299 ± 0.011
^{113}Ag	5.37 h	298.6	10.0	0.287 ± 0.044	0.287 ± 0.044
^{115}Cd^{g}	53.46 h	336.2	45.9	0.245 ± 0.016	0.244 ± 0.016
^{115}Cd^{total}				$0.284 \pm 0.016^{*}$	$0.284 \pm 0.016^{*}$
^{117}Cd^{m}	3.36 h	1066.0	23.1	$.0290 \pm .0011$	
		1097.3	26.0	$.0268 \pm .0016$	
^{117}Cd^{g}	2.49 h	273.4	28.0	$.2352 \pm .0219$	
^{117}Cd^{total}				$.2631 \pm .0230$	$.2631 \pm .0230$
^{127}Sb	3.85 d	687.0	37.0	0.656 ± 0.027	0.656 ± 0.027
^{128}Sn	59.07 min	482.3	59.0	0.963 ± 0.044	0.986 ± 0.045
^{129}Sb	4.32 h	812.4	43.0	1.417 ± 0.071	1.417 ± 0.071
^{131}Sb	23.03 min	943.4	47.0	4.239 ± 0.223	
^{131}I	8.02 d	364.5	81.7	4.442 ± 0.186	4.442 ± 0.186
^{132}Te	3.2 d	228.1	88.0	5.661 ± 0.153	5.673 ± 0.153
^{133}I	20.8 h	529.9	87.0	6.811 ± 0.208	6.811 ± 0.208
^{134}Te	41.8 min	566.0	18.0	6.854 ± 0.294	7.891 ± 0.339
		767.2	29.5	7.199 ± 0.267	8.293 ± 0.308
^{134}I	52.5 min	847.0	95.4	8.168 ± 0.367	8.168 ± 0.367
		884.1	65.0	8.225 ± 0.197	8.225 ± 0.197
^{135}I	6.57 h	1131.5	22.7	5.514 ± 0.266	5.607 ± 0.271
		1260.4	28.9	5.470 ± 0.054	5.563 ± 0.055
^{137}Xe	3.7 min	455.5	310	6.788 ± 0.213	6.788 ± 0.213
^{138}Cs^{g}	33.41 min	1435.8	76.3	6.876 ± 0.228	6.890 ± 0.228
		1009.8	29.8	6.980 ± 0.295	6.994 ± 0.295
		462.8	30.7	6.931 ± 0.283	6.945 ± 0.283
^{139}Ba	83.03 min	165.8	23.7	5.564 ± 0.284	5.564 ± 0.284
^{140}Ba	12.75 d	537.3	24.4	4.929 ± 0.142	4.929 ± 0.142
^{141}Ba	18.27 min	190.3	46.0	4.160 ± 0.213	
		304.7	35.4	4.125 ± 0.201	

Table 4. Continued.

Nuclide	Half-life	γ-ray Energy (keV)	abundance γ-ray (%)	Y_R (%)	Y_A (%)
^{141}Ce	32.5 d	145.4	48.0	4.327 ± 0.234	4.327 ± 0.234
^{142}Ba	10.6 min	255.3	20.5	4.502 ± 0.137	
^{142}La	91.1 min	641.3	47.0	4.534 ± 0.284	4.534 ± 0.284
^{143}Ce	33.03 h	293.3	42.8	4.834 ± 0.219	4.834 ± 0.219
^{144}Ce	284.89 d	133.5	11.09	4.245 ± 0.186	4.245 ± 0.186
^{146}Ce	13.52 min	316.7	56.0	2.713 ± 0.191	
		218.2	20.6	3.047 ± 0.153	
^{146}Pr	24.15 min	453.9	48.0	3.206 ± 0.186	3.206 ± 0.186
		1524.7	15.6	3.227 ± 0.121	3.227 ± 0.121
^{147}Nd	10.98 d	531.0	13.1	2.407 ± 0.137	2.407 ± 0.137
^{149}Nd	1.728 h	211.3	25.9	1.165 ± 0.033	
		270.2	10.6	1.182 ± 0.022	
^{149}Pm	53.08 h	286.0	3.1	1.312 ± 0.038	1.312 ± 0.038
^{151}Pm	53.08 h	340.8	23.0	0.749 ± 0.028	0.749 ± 0.028
^{153}Sm	46.28 h	103.2	30.0	0.323 ± 0.017	0.323 ± 0.017

(a) Y_R – Cumulative yields.
(b) Y_A – Mass yields.
(c) The yields of ^{115}Cd$^{\text{total}}$ is based on the ratio of ^{115}Cd$^{\text{g}}$/^{115}Cd$^{\text{m}}$ = 6 from ref. [38].
(d) ^{135}I – Fission rate monitor.

ical $82n$ shell if the neutron emission is around one. Similarly, around mass number 138–39 and 143–144, the most probable Z is 54 and 56, then the fission fragment has deformed 86–88n shell if the neutron emission is around one or two. Besides this, the deformed neutron shell around 88 and 64 lie between the neutron numbers 86–90 and 62–66, respectively [75]. In the case of ^{238}U(γ, f) and ^{238}U(n, f), for the fragment of $A = 134$, they have the complementary fragment around $A = 104$ and 105 with probable $Z = 40$. Thus the probable neutrons for the complementary pairs have the spherical $82n$ and deformed $64n$ shell combination in ^{238}U(γ, f). Thus the slightly higher yield of the fission products with $A = 133$–134 and their complementary in ^{238}U(γ, f) compared to ^{238}U(n, f) is due to the spherical $82n$ and the deformed $64n$ shell combination in the former rather than in the latter. Similarly, in ^{238}U(n, f), the fragment of $A = 139$ has the complementary fragment around $A = 100$ with probable $Z = 38$. Then the probable neutrons for the complementary pairs have deformed $86n$ and $62n$ shell combination. Thus the fission products for $A = 138$ and 98 in ^{238}U(n, f) have unusual high yields around 11% [21]. The difference of one neutron between the fissioning systems ^{238}U* and ^{239}U* seems not so reasonable for the unusually different yield for the fission products of $A = 138$ and its complementary. However, this fact gets support from the observation of very high yields of 10.85% for $A = 144$ and 84 in ^{229}Th(n, f) [85] but not as high as in ^{232}Th(γ, f) [86]. The higher yields for $A = 144$ and 84 in ^{229}Th(n, f) [85] are due to the deformed $88n$ and spherical $50n$ shell combination. Besides the shell combination, the higher yields for $A = 133$–134 and 138–139 in ^{238}U(γ, f) and ^{238}U(n, f) with most probable Z of 54 and 56 are also favorable from the N/Z ratio between complementary fragments and fissioning systems. The fissioning systems ^{238}U* and ^{239}U* have a N/Z ratios of 1.587 and 1.598, respectively. For the fission products with $A = 134$ and 138 have the N/Z ratios of 1.596 and 1.593, in their fragment stage, are based on the emission of one and two neutrons, respectively. This is based on the probable neutron-to-proton ratios of 82/52 and 86/54, respectively. Thus the higher yields of products around $A = 133$–134 and 138–139 in ^{238}U(γ, f) and ^{238}U(n, f) are favorable from the N/Z ratio besides the presence of the deformed $82n$ and $64n$ or $86n$ and $62n$ shell combination in the fragment stage. For the fission product of $A = 144$, the N/Z ratio is 1.607 by considering the two-neutron emission. The N/Z value of 1.607 is higher than the value of 1.587 and 1.598 of the fission systems ^{238}U* and ^{239}U*. Besides this the complementary pairs do not have shell combination. So the yield of fission products for $A = 143$–144 are lower than those of the fission products for $A = 133$–34 and 138–139 for both the fissioning systems.

Further, from fig. 5, it can be seen that the yields of the fission products for $A = 134$, 139 and 143 decrease with excitation energy. This is due to the decrease of the even-odd effect with excitation energy [68,86]. The effect of the excitation energy can be seen in a better way from the yields of the symmetric fission products and the peak-to-valley (P/V) ratio. Thus the yields of high-yield asymmetric products, the yields of symmetric products and their peak-to-valley (P/V) ratio in the bremsstrahlung-induced fission of ^{238}U from the present work and the literature data [52–72] as a function of the excitation en-

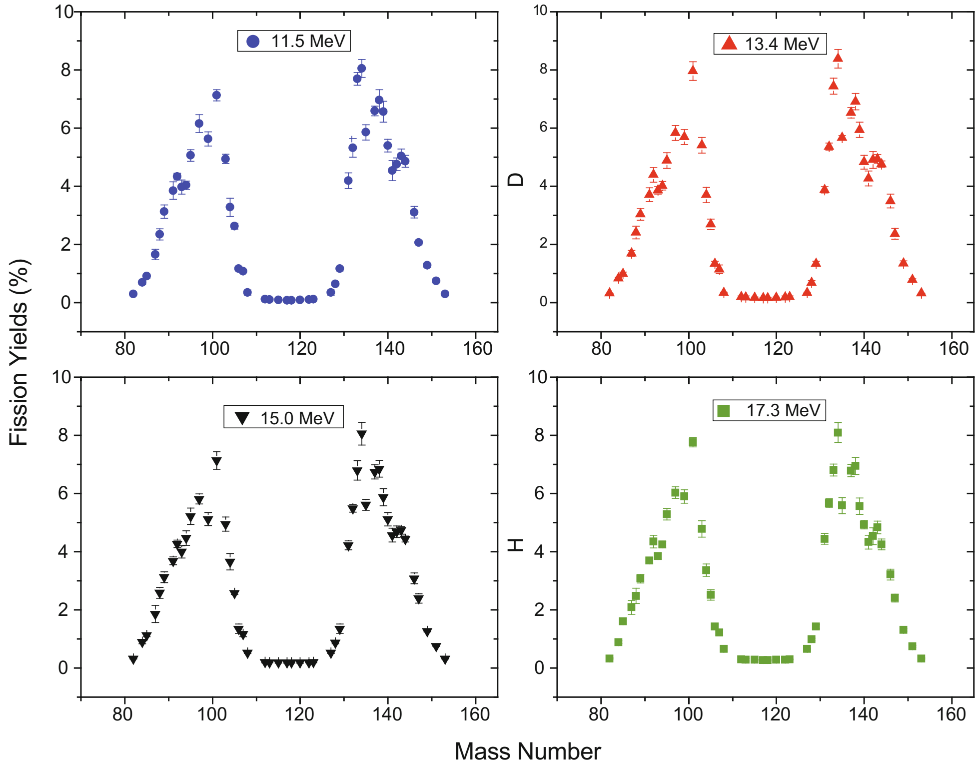

Fig. 3. Plot of the mass yields distribution in the 11.5, 13.4, 15.0 and 17.3 MeV bremsstrahlung-induced fission of ^{238}U.

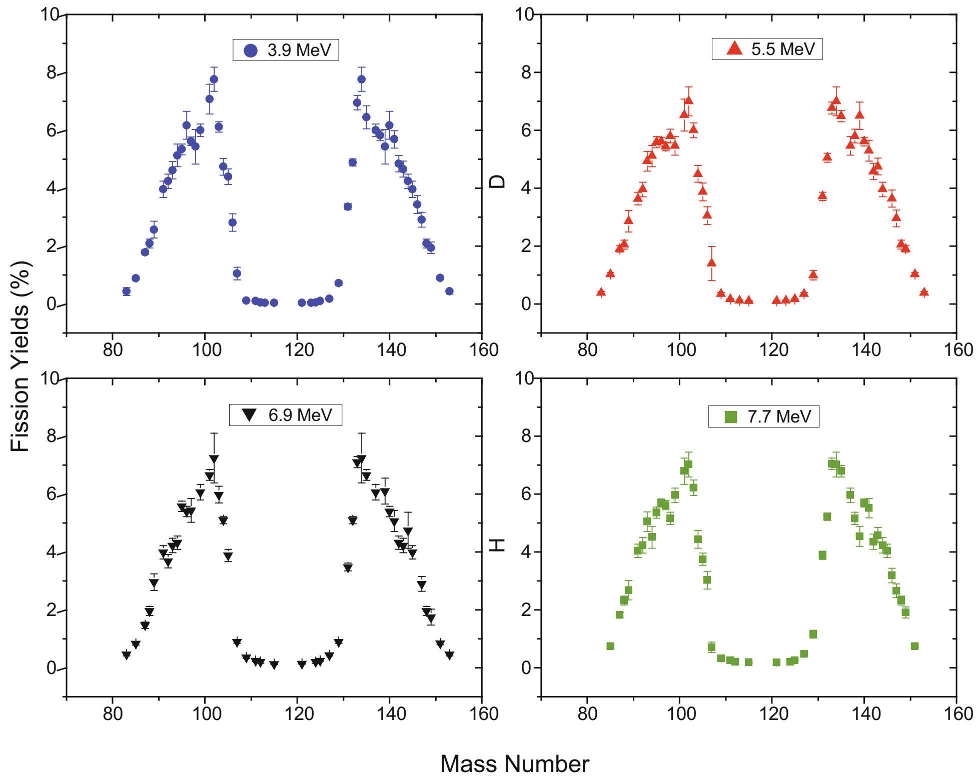

Fig. 4. Plot of the mass yields distribution in the 3.9, 5.5, 6.9 and 7.7 MeV neutron-induced fission of ^{238}U.

Table 5. Yields of asymmetric (Y) products for $A = 133$–134, 139–140 and 143–144 in the bremsstrahlung-induced fission of ^{238}U.

E_γ (MeV)	E^* (MeV)	Y (%) 133–134	Y(%)139–140	Y(%)143–144	Reference
6.12	5.55	7.660 ± 0.383	6.620 ± 0.331	4.580 ± 0.229	[68]
		8.570 ± 0.429	5.700 ± 0.285	4.870 ± 0.244	
6.44	5.86	7.970 ± 0.399	6.560 ± 0.328	4.900 ± 0.245	[68]
		8.340 ± 0.417	6.040 ± 0.302	4.930 ± 0.247	
7.33	6.23	8.430 ± 0.422	7.130 ± 0.357	4.410 ± 0.221	[68]
		8.380 ± 0.419	6.440 ± 0.322	4.980 ± 0.249	
8.35	6.68	8.210 ± 0.411	6.340 ± 0.317	4.980 ± 0.249	[68]
		8.430 ± 0.419	6.060 ± 0.303	4.620 ± 0.231	
9.31	7.19	7.860 ± 0.393	6.510 ± 0.326	4.990 ± 0.250	[68]
		7.690 ± 0.385	6.240 ± 0.312	4.750 ± 0.238	
10.0	7.55	7.429 ± 0.801	5.999 ± 0.114	4.273 ± 0.292	[72]
		8.266 ± 0.297	5.401 ± 0.293	4.786 ± 0.269	
10.0	7.55	6.800 ± 0.600	5.870 ± 0.470	5.940 ± 0.475	[53]
		–	5.770 ± 0.470	–	
11.1	8.4	7.710 ± 0.389	6.240 ± 0.312	5.110 ± 0.256	[68]
		7.730 ± 0.387	6.030 ± 0.302	4.890 ± 0.245	
11.5	9.09	7.688 ± 0.217	6.565 ± 0.362	5.035 ± 0.250	Present work
		7.463 ± 0.289	5.396 ± 0.217	4.863 ± 0.206	
12.0	9.7	6.800 ± 0.340	–	4.800 ± 0.340	[64]
		6.880 ± 0.230	5.930 ± 0.214	4.600 ± 0.320	
13.4	10.38	7.425 ± 0.271	5.941 ± 0.259	4.940 ± 0.146	Present work
		7.659 ± 0.289	4.828 ± 0.236	4.759 ± 0.108	
15.0	11.6	6.791 ± 0.334	5.871 ± 0.295	4.738 ± 0.195	Present work
		7.231 ± 0.345	5.118 ± 0.229	4.437 ± 0.106	
15.0	11.6	6.340 ± 0.370	–	4.720 ± 0.340	[64]
		6.870 ± 0.250	5.910 ± 0.200	4.240 ± 0.460	
16.0	12.4	7.060 ± 0.400	5.970 ± 0.358	5.320 ± 0.340	[53]
		–	5.770 ± 0.330	–	
17.3	12.71	6.811 ± 0.208	5.564 ± 0.284	4.834 ± 0.219	Present work
		7.027 ± 0.294	4.929 ± 0.142	4.245 ± 0.186	
20.0	13.4	6.300 ± 0.350	–	4.530 ± 0.320	[64]
		6.840 ± 0.220	5.590 ± 0.200	3.970 ± 0.340	
21.0	13.6	–	–	4.000 ± 0.100	[52]
		–	4.900 ± 0.100	3.800 ± 0.200	
22.0	13.85	5.610 ± 0.390	–	5.670 ± 0.400	[60]
		–	5.000 ± 0.350	–	
25.0	14.38	6.600 ± 0.528	6.870 ± 0.550	4.510 ± 0.361	[59]
		5.320 ± 0.426	5.530 ± 0.442	3.180 ± 0.254	
25.0	14.38	6.310 ± 0.320	–	4.510 ± 0.330	[62]
		6.590 ± 0.330	5.390 ± 0.220	4.240 ± 0.310	
30.0	14.7	5.930 ± 0.474	6.250 ± 0.500	4.650 ± 0.372	[59]
		–	5.480 ± 0.438	3.270 ± 0.262	
30.0	14.7	6.100 ± 0.310	–	4.390 ± 0.310	[64]
		6.430 ± 0.210	5.620 ± 0.180	3.820 ± 0.320	

Table 5. Continued.

E_γ (MeV)	E^* (MeV)	Y (%) 133–134	Y(%)139–140	Y(%)143–144	Reference
35.0	15.08	6.900 ± 0.552	6.060 ± 0.485	4.030 ± 0.322	[59]
		5.450 ± 0.436	4.970 ± 0.398	–	
40.0	15.58	6.580 ± 0.526	5.970 ± 0.478	4.400 ± 0.352	[59]
		–	5.150 ± 0.412	3.470 ± 0.278	
48.0	16.22	6.200 ± 0.300	4.600 ± 0.100	3.800 ± 0.300	[52]
		–	5.000 ± 0.300	3.400 ± 0.200	
70.0	11.87	5.840 ± 0.300	–	4.200 ± 0.320	[64]
		6.120 ± 0.270	5.330 ± 0.170	3.650 ± 0.260	

ergy are shown in table 7. Similarly, the yields of high-yield asymmetric products, yields of symmetric products and their P/V ratio in the neutron-induced fission of ^{238}U from the literature data [23–48] as a function of the excitation energy are shown in table 8 for comparison. In the ^{238}U(γ, f) and ^{238}U(n, f), the yield of high-yield asymmetric products is $A = 133$ or 134 and, for the symmetric product, it is for $A = 115$ or 117 depending upon the availability of data in the literature. The yields of high-yield asymmetric products and the yields of symmetric products in the bremsstrahlung- and neutron-induced fission of ^{238}U as a function of the excitation energy from tables 7 and 8 are plotted in fig. 6. Similarly, the P/V ratio in the bremsstrahlung- and neutron-induced fission of ^{238}U as a function of the excitation energy from tables 7 and 8 are plotted in fig. 7. It can be seen from fig. 6 that, in both ^{238}U(γ, f) and ^{238}U(n, f), the yields of the high-yield asymmetric products decrease marginally with excitation energy. However, the yields of the symmetric fission products increase significantly with excitation energy. Accordingly, the peak-to-valley (P/V) ratio decreases with excitation energy in both the bremsstrahlung- and the neutron-induced fission of ^{238}U (fig. 7). The increase of the symmetric-product yield (fig. 6) and the decrease of the P/V ratio (fig. 7) clearly indicate the effect of the excitation energy. Further, it can be seen, from fig. 6, that at the same excitation energy, the yields of the symmetric products are slightly higher in the ^{238}U(γ, f) than in the ^{238}U(n, f). These causes a slightly lower P/V ratio in the ^{238}U(γ, f) than in the ^{238}U(n, f) (fig. 7). Besides the role of the excitation energy, the difference may be due to the slightly lower height of the outer fission barrier of 5.7 MeV in the fissioning system ^{238}U* compared to 6.12 MeV in ^{239}U* [87]. The role of the excitation energy above the outer fission barrier is clearly shown by Pomme *et al.* [68]. It was shown by them that the proton odd-even effect is nearly constant up to the excitation energy of 2.2 MeV above the outer barrier. The lower height of the outer fission barrier in the fissioning system ^{238}U* compared to ^{239}U* is due to the pairing effect.

The role of the excitation energy and the pairing effect can also be seen from the average heavy mass ($\langle A_\mathrm{H} \rangle$), light mass ($\langle A_\mathrm{L} \rangle$) and neutron number ($\langle v \rangle$). In order to examine this, the $\langle A_\mathrm{L} \rangle$ and $\langle A_\mathrm{H} \rangle$ in the bremsstrahlung-induced fission of ^{238}U at 11.5, 13.4, 15.0 and 17.3 MeV from the present work and at other energies from the literature [52–72] are calculated from the mass chain yields (Y_A) of the fission products within the mass ranges of 80–105 and 125–150 by using the following relation [64]:

$$\langle A_L \rangle = \frac{\Sigma(Y_A A_L)}{\Sigma Y_A}, \quad \langle A_H \rangle = \frac{\Sigma(Y_A A_{LH})}{\Sigma Y_A}. \qquad (8)$$

The $\langle A_\mathrm{L} \rangle$ and $\langle A_\mathrm{H} \rangle$ values obtained from the above relation in the bremsstrahlung-induced fission of ^{238}U, along with their corresponding average excitation energy ($\langle E^* \rangle$) from the present work and the literature [52–72], are given in table 9. Similarly, the $\langle A_\mathrm{L} \rangle$ and $\langle A_\mathrm{H} \rangle$ values in the neutron-induced fission of ^{238}U along with their corresponding average excitation energy ($\langle E^* \rangle$) from the literature [23–48] are given in table 10 for comparison. From the compound nucleus mass ($A_\mathrm{C} = 238$), and from the$\langle A_\mathrm{L} \rangle$ and $\langle A_\mathrm{H} \rangle$ values, the experimental average number of neutrons ($\langle v \rangle_\mathrm{expt}$) was calculated using the following relation [69]:

$$\langle v \rangle_{expt} = A_C - (\langle A_L \rangle + \langle A_H \rangle). \qquad (9)$$

The $\langle v \rangle_\mathrm{expt}$ values obtained from the above relation in the bremsstrahlung- and neutron-induced fission of ^{238}U at different excitation energies are listed in tables 9 and 10, respectively. The average neutron number ($\langle v \rangle_\mathrm{calc}$) at different excitation energies in ^{238}U(γ, f) was also calculated as done earlier [86] in ^{232}Th(γ, f) based on the assumption that the average energy needed for the emission of neutron is 8.6 MeV [88]. The total excitation energy ($\langle E^*_\mathrm{tot} \rangle$) at the scission point used in the calculation of average neutron numbers ($\langle v \rangle_\mathrm{calc}$) is obtained from the average Q-value ($\langle Q \rangle$), average kinetic energy ($\langle E_\mathrm{K} \rangle$), and average excitation energy ($\langle E^* \rangle$) as follows [86]:

$$\langle E^*_{tot} \rangle = \langle Q \rangle - \langle E_K \rangle + \langle E^* \rangle. \qquad (10)$$

Table 6. Yields of asymmetric (Y) products for $A = 133$–134, 139–140 and 143–144 in the neutron-induced fission of ^{238}U.

E_n (MeV)	E^* (MeV)	Y (%) 133–134	Y(%)139–140	Y(%)143–144	Reference
1.5	5.85	7.150 ± 0.220	7.110 ± 0.710	4.630 ± 0.290	[38]
		8.120 ± 0.400	6.010 ± 0.180	–	[38]
1.72	6.07	7.080 ± 0.710	–	4.590 ± 0.550	[42]
		6.640 ± 0.740	5.720 ± 0.360	–	
2.0	6.35	7.120 ± 0.210	6.950 ± 0.550	4.650 ± 0.250	[38]
		7.780 ± 0.370	6.100 ± 0.130	–	
2.16	6.55	6.960 ± 0.720	–	4.490 ± 0.490	[42]
		6.540 ± 0.710	5.760 ± 0.310	–	
3.0	7.35	7.370 ± 0.820	6.510 ± 0.610	5.450 ± 0.500	[33]
		8.190 ± 0.840	6.160 ± 0.130	–	
3.72	8.07	6.500 ± 0.670	–	4.390 ± 0.450	[42]
		6.110 ± 0.750	5.560 ± 0.360	–	
3.72	8.07	6.977 ± 0.587	6.537 ± 0.209	4.592 ± 0.297	[48]
		7.945 ± 0.267	5.684 ± 0.291	4.847 ± 0.255	
3.9	8.25	6.950 ± 0.250	5.430 ± 0.600	4.660 ± 0.270	[38]
		7.760 ± 0.420	6.170 ± 0.480	–	
4.78	9.13	6.170 ± 0.630	5.330 ± 0.710	4.470 ± 0.460	[42]
		6.640 ± 0.400	6.140 ± 0.450	–	
5.42	9.77	6.341 ± 0.211	6.604 ± 0.273	4.912 ± 0.121	[48]
		7.223 ± 0.277	5.930 ± 0.214	5.211 ± 0.178	
5.0	9.35	6.932 ± 0.912	5.893 ± 0.811	4.698 ± 0.609	[45]
		7.112 ± 1.006	5.984 ± 0.778	–	
5.5	9.85	6.770 ± 0.200	6.500 ± 0.470	4.750 ± 0.290	[38]
		7.000 ± 0.500	5.610 ± 0.150	–	
5.98	10.33	6.940 ± 0.760	–	4.640 ± 0.550	[42]
		5.310 ± 0.610	5.850 ± 0.400	–	
6.0	10.35	6.132 ± 0.699	–	4.333 ± 0.377	[37]
		–	5.384 ± 0.291	4.326 ± 0.242	
6.9	11.25	7.100 ± 0.190	6.100 ± 0.450	4.280 ± 0.260	[38]
		7.240 ± 0.860	5.400 ± 0.180	4.750 ± 0.620	
7.1	11.45	6.839 ± 0.595	–	4.691 ± 0.282	[37]
		–	5.346 ± 0.294	5.080 ± 0.295	
7.7	12.05	7.040 ± 0.200	4.540 ± 0.540	4.580 ± 0.270	[38]
		7.020 ± 0.430	4.827 ± 0.204	–	
7.75	12.1	6.818 ± 0.243	6.484 ± 0.124	4.698 ± 0.195	[48]
		7.257 ± 0.215	6.011 ± 0.258	4.827 ± 0.204	
8.1	12.45	6.713 ± 0.665	–	4.775 ± 0.282	[37]
		–	5.146 ± 0.309	4.689 ± 0.609	
8.27	12.72	7.210 ± 0.220	4.890 ± 0.300	4.660 ± 0.140	[43]
		6.550 ± 0.230	5.710 ± 0.170	4.060 ± 0.120	
9.1	13.45	6.308 ± 0.688	–	4.370 ± 0.323	[37]
		–	4.982 ± 0.379	4.272 ± 0.312	
10.09	14.55	6.501 ± 0.176	5.889 ± 0.344	4.471 ± 0.199	[48]
		6.785 ± 0.286	5.449 ± 0.232	4.641 ± 0.206	

Table 6. Continued.

E_n (MeV)	E^* (MeV)	Y (%) 133–134	Y(%)139–140	Y(%)143–144	Reference
11.3	15.65	6.660 ± 0.260	5.100 ± 0.300	4.280 ± 0.160	[43]
		6.280 ± 0.270	5.000 ± 0.190	–	
14.0	18.10	6.080 ± 0.140	5.020 ± 0.330	4.260 ± 0.440	[26]
		6.500 ± 0.150	4.540 ± 0.530	4.689 ± 0.609	
14.1	18.45	5.730 ± 0.370	5.100 ± 0.320	3.830 ± 0.250	[35]
		5.490 ± 0.450	4.600 ± 0.400	3.620 ± 0.190	
14.4	18.75	6.130 ± 0.320	5.130 ± 0.250	3.850 ± 0.090	[36]
		6.340 ± 0.340	4.890 ± 0.270	3.390 ± 0.220	
14.5	18.85	–	4.910 ± 0.300	–	[32]
		–	4.860 ± 0.300	–	
14.7	19.05	6.360 ± 0.450	4.400 ± 0.500	4.320 ± 0.350	[39]
		5.630 ± 0.560	4.560 ± 0.214	4.000 ± 0.530	[46]
14.8	19.15	5.680 ± 0.510	5.440 ± 0.410	4.250 ± 0.100	[34]
		6.350 ± 0.300	4.540 ± 0.400	3.820 ± 0.300	[29]
14.9	19.25	6.000 ± 0.190	4.620 ± 0.214	4.200 ± 0.140	[41]
		6.500 ± 0.200	4.590 ± 0.150	4.010 ± 0.210	

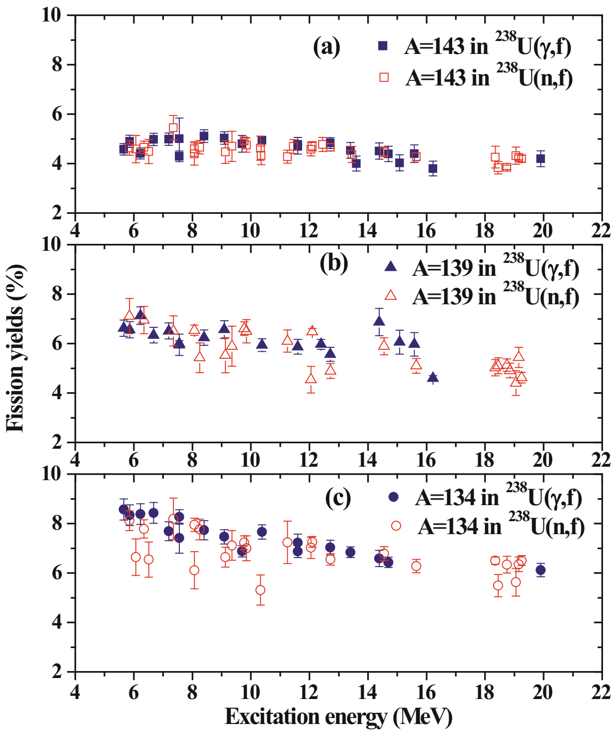

Fig. 5. Plot of the yields of fission products (%) as a function of the excitation energy for $A = 143$, 139 and 134 in the ^{238}U(γ, f) and ^{238}U(n, f) reactions.

From the experimental work of Jacobs *et al.* [65] and Pomme *et al.* [69], it can be seen that the difference between$\langle Q \rangle$ and $\langle E_{\mathrm{K}} \rangle$ is around 16.5 MeV throughout the bremsstrahlung energy region from 6.12 to 70 MeV. The $\langle v \rangle_{\mathrm{calc}}$ value obtained based on the above assumption is listed in table 9, which is found to be in good agreement with the experimental value. The $\langle v \rangle_{\mathrm{expt}}$ values for ^{238}U(γ, f) from table 9 and those for ^{238}U(n, f) from table 10 are plotted in fig. 8 as a function of the excitation energy. It can be seen, from fig. 8, that in both the bremsstrahlung- and the neutron-induced fission of ^{238}U, the values of $\langle v \rangle_{\mathrm{expt}}$ increase in a similar way, which indicates the role of the excitation energy. However, within excitation energy of 12.5 MeV, the average neutron number in the ^{238}U(n, f) reaction is lower than in ^{238}U(γ, f). Beyond the excitation energy of 12.5 MeV, the average neutron number is slightly higher in ^{238}U(n, f) than in ^{238}U(γ, f). This is because the average neutron number increases faster with excitation energy in ^{238}U(n, f) than in ^{238}U(γ, f). This indicates that the partition of the excitation energy between collective and intrinsic degrees of freedom [75] is different for photon- and neutron-induced fission of ^{238}U. This reflects in the yield profiles and thus in the average$\langle A_{\mathrm{L}} \rangle$ and $\langle A_{\mathrm{H}} \rangle$ values.

In order to examine the above aspects, the $\langle A_{\mathrm{L}} \rangle$ and $\langle A_{\mathrm{H}} \rangle$ values for the ^{238}U(γ, f) reaction from table 9 and for the ^{238}U(n, f) reaction from table 10 are plotted in fig. 9. It can be seen from fig. 9 that the $\langle A_{\mathrm{H}} \rangle$ value for

Table 7. Yields of asymmetric (Y_a, $A = 133$–134) and symmetric (Y_s, $A = 115$–117) products and P/V ratio in the bremsstrahlung-induced fission of ^{238}U.

E_n (MeV)	E^* (MeV)	Y_a (%)	Y_s (%)	P/V	Reference
6.12	5.66	8.570 ± 0.429	–	–	[68]
6.44	5.84	8.340 ± 0.417	–	–	[68]
7.33	6.23	8.380 ± 0.419	–	–	[68]
8.35	6.68	8.430 ± 0.422	–	–	[68]
9.0	6.86	7.140 ± 0.660	0.023 ± 0.006	310.4 ± 85.9	[52]
9.31	7.19	7.690 ± 0.385	–	–	[68]
10.0	7.55	6.800 ± 0.600	0.033 ± 0.007	206.9 ± 47.7	[53]
10.0	7.55	8.821 ± 0.709	0.046 ± 0.002	192.0 ± 17.5	[72]
11.1	8.4	7.730 ± 0.387	–	–	[68]
11.5	9.09	7.463 ± 0.289	0.074 ± 0.006	100.7 ± 9.1	Present work
12.0	9.7	6.880 ± 0.230	0.075 ± 0.007	78.0 ± 7.0	[64]
13.4	10.38	7.659 ± 0.289	0.154 ± 0.023	49.7 ± 7.7	Present work
15.0	11.6	7.231 ± 0.345	0.188 ± 0.023	38.5 ± 5.0	Present work
15.0	11.6	6.870 ± 0.250	0.172 ± 0.021	31.0 ± 2.0	[64]
16.0	12.4	6.600	0.173 ± 0.010	38.0	[53]
17.3	12.71	7.027 ± 0.294	0.263 ± 0.023	26.7 ± 2.6	Present work
20.0	13.4	6.840 ± 0.220	0.281 ± 0.031	24.3 ± 2.8	[64]
21.0	13.6	6.600	0.268 ± 0.020	23.0	[52]
22.0	13.85	6.900 ± 0.500	0.315 ± 0.055	20.0	[60]
25.0	14.38	6.590 ± 0.330	0.334 ± 0.032	19.0 ± 2.0	[62]
25.0	14.38	–	0.440 ± 0.060	–	[57]
25.0	14.38	6.870 ± 0.550	0.475 ± 0.038	16.0 ± 0.5	[59, 64]
30.0	14.7	6.430 ± 0.210	0.446 ± 0.045	13.0 ± 0.5	[64]
30.0	14.7	6.610 ± 0.529	0.522 ± 0.042	12.0	[59]
35.0	15.08	6.180 ± 0.494	0.529 ± 0.042	11.4	[59]
40.0	15.58	6.020 ± 0.482	0.542 ± 0.043	10.6	[59]
48.0	16.22	6.200 ± 0.300	0.600 ± 0.020	11.0	[52]
70.0	19.9	6.120 ± 0.270	0.737 ± 0.064	8.5 ± 0.3	[64]

the ^{238}U(γ, f) reaction increases slightly within the excitation energy of 2.2 MeV above the outer barrier and then remains almost constant. Thus the average $\langle A_{\mathrm{H}} \rangle$ value for the ^{238}U(γ, f) reaction is around 137.59 ± 0.21. For the ^{238}U(n, f) reaction, with the increase of the excitation energy, the $\langle A_{\mathrm{H}} \rangle$ value decreases from 139 to 137. The lower and near constant $\langle A_{\mathrm{H}} \rangle$ value of 137.59 ± 0.21 is due to the slightly higher yield of the fission products around mass number 133–134 in the ^{238}U(γ, f) reaction than in the ^{238}U(n, f) reaction, which was mentioned before based on fig. 5. Accordingly, with the increase of the excitation energy, the $\langle A_{\mathrm{L}} \rangle$ value for the ^{238}U(γ, f) reaction decreases from 98 to 96. In the ^{238}U(n, f) reaction, the yields of the fission products around mass numbers 133–134 increase with the excitation energy, which was earlier mentioned from fig. 5. Thus the $\langle A_{\mathrm{H}} \rangle$ value in the ^{238}U(n, f) reaction, decreases with the excitation energy from 139 to 137. Accordingly, with the increase of the excitation energy, the $\langle A_{\mathrm{L}} \rangle$ value for the ^{238}U(n, f) reaction remains nearly constant or increases slowly from 97.5 to 98. The increase or decrease trend of the$\langle A_{\mathrm{L}} \rangle$ and $\langle A_{\mathrm{H}} \rangle$ values with excitation energy in the ^{238}U(γ, f) and ^{238}U(n, f) reactions are due to the mass conservation of the fissioning system. However, the surprising different behavior of the $\langle A_{\mathrm{L}} \rangle$ and $\langle A_{\mathrm{H}} \rangle$ values with excitation energy between the ^{238}U(γ, f) and ^{238}U(n, f) reactions is not only based on the mass conservation of the fissioning system but it is also due to the different role of the standard I and II asymmetric modes of the fission [74] and the shell combination [75] of the complementary fragments. This indicates that the role of standard I and II asymmetric modes of the fission is different between the ^{238}U(γ, f) and ^{238}U(n, f) reactions based on the shell combination of the complementary fragments. This also indicates that the potential energy surface is different between the ^{238}U(γ, f) and ^{238}U(n, f) reactions due to the single odd-nucleon in the later.

Table 8. Yields of asymmetric (Y_a) and symmetric (Y_s) products and P/V ratio in neutron-induced fission of ^{238}U.

E_n (MeV)	E^* (MeV)	Y_a (%)	Y_s (%)	P/V	Reference
1.5	5.85	8.120 ± 0.400	0.0102 ± 0.0014	796.1 ± 116.1	[38]
1.5	5.85	–	0.0075 ± 0.0008	825.0	[25]
1.72	6.07	7.830 ± 0.930	–	–	[42]
2.0	6.35	7.780 ± 0.370	0.0121 ± 0.0017	643.0 ± 95.4	[38]
2.0	6.35	–	0.0135 ± 0.0014	452.0	[25]
2.16	6.55	7.510 ± 0.830	–	–	[42]
3.0	7.35	–	0.029 ± 0.003	238.0	[25]
3.0	7.35	8.190 ± 0.840	0.034 ± 0.006	240.9 ± 49.2	[33]
3.72	8.07	7.945 ± 0.267	0.038 ± 0.006	209.1 ± 33.7	[48]
3.72	8.07	7.490 ± 0.790	–	–	[42]
3.9	8.25	7.760 ± 0.420	0.034 ± 0.005	228.2 ± 35.8	[38]
3.9	8.25	–	0.047 ± 0.005	129.0	[25]
4.78	9.13	6.770 ± 0.700	–	–	[42]
4.8	9.15	–	0.068 ± 0.007	89.0	[25]
5.42	9.77	7.223 ± 0.277	0.074 ± 0.018	97.6 ± 24.1	[48]
5.5	9.85	7.000 ± 0.500	0.077 ± 0.011	90.9 ± 14.5	[38]
5.98	10.33	6.290 ± 0.800	–	–	[42]
6.0	10.35	6.132 ± 0.699	0.124 ± 0.010	49.5 ± 6.9	[37]
6.9	11.25	7.240 ± 0.860	0.134 ± 0.018	54.0 ± 9.7	[38]
7.1	11.45	6.839 ± 0.595	0.121 ± 0.009	56.5 ± 6.5	[37]
7.7	12.05	7.020 ± 0.430	0.191 ± 0.032	36.8 ± 6.6	[38]
7.75	12.1	7.257 ± 0.215	0.202 ± 0.037	35.9 ± 6.7	[48]
8.1	12.45	6.713 ± 0.665	0.135 ± 0.011	49.7 ± 6.4	[37]
8.27	12.72	7.210 ± 0.430	0.227 ± 0.009	31.2 ± 1.6	[40]
9.1	13.45	6.308 ± 0.688	0.191 ± 0.016	33.0 ± 4.5	[37]
10.09	14.55	6.785 ± 0.286	0.338 ± 0.039	20.1 ± 2.5	[48]
11.3	15.65	6.660 ± 0.260	0.430 ± 0.050	15.5 ± 1.9	[43]
13.0	17.35	–	0.570 ± 0.070	8.8	[25]
14.0	18.35	6.500 ± 0.150	0.860 ± 0.090	7.6 ± 0.8	[26]
14.0	18.35	–	0.970 ± 0.150	–	[35]
14.1	18.45	6.000 ± 0.210	0.950 ± 0.090	6.6 ± 0.6	[32]
14.4	18.75	6.340 ± 0.340	0.843 ± 0.048	7.5 ± 0.6	[36]
14.4	18.75	–	0.975 ± 0.055	–	[36]
14.7	19.05	6.360 ± 0.450	0.860 ± 0.090	7.4 ± 0.9	[57]
14.7	19.05	–	0.930 ± 0.120	–	[57]
14.8	19.15	6.350 ± 0.300	0.870 ± 0.150	7.3 ± 1.3	[34]
14.8	19.15	–	0.950 ± 0.070	–	[34]
14.9	19.25	6.50 ± 0.300	0.985 ± 0.039	6.6 ± 0.4	[41]
14.9	19.05	–	0.834 ± 0.039	–	[41]
15.0	19.35	–	0.780 ± 0.090	6.5	[25]
16.4	20.75	–	0.870 ± 0.100	5.8	[25]
17.7	22.05	–	0.740 ± 0.090	6.8	[25]

Table 9. Average light mass ($\langle A_L \rangle$), heavy mass ($\langle A_H \rangle$), and average neutron numbers ($\langle v \rangle_{expt}$ and $\langle v \rangle_{calc}$) in the bremsstrahlung-induced fission of ^{238}U.

E_γ (MeV)	E^* (MeV)	$\langle A_L \rangle$	$\langle A_H \rangle$	$\langle v \rangle_{expt}$	$\langle v \rangle_{cal}$	Reference
6.12	5.66	98.06 ± 0.14	137.38 ± 0.15	2.56 ± 0.15	2.58	[68]
6.44	5.84	98.08 ± 0.14	137.40 ± 0.15	2.52 ± 0.15	2.59	[68]
7.33	6.23	97.95 ± 0.14	137.40 ± 0.15	2.65 ± 0.15	2.64	[68]
8.35	6.68	97.81 ± 0.14	137.45 ± 0.15	2.74 ± 0.15	2.69	[68]
9.31	7.19	97.75 ± 0.14	137.55 ± 0.15	2.70 ± 0.15	2.75	[68]
10.0	7.55	97.68 ± 0.15	137.60 ± 0.15	2.72 ± 0.15	2.79	[72]
11.1	8.4	97.67 ± 0.14	137.54 ± 0.15	2.79 ± 0.15	2.89	[68]
11.5	9.09	97.45 ± 0.16	137.68 ± 0.08	2.87 ± 0.16	2.97	Present work
12.0	9.7	97.25 ± 0.08	137.87 ± 0.07	2.85 ± 0.11	3.04	[64]
13.4	10.38	97.26 ± 0.12	137.65 ± 0.08	3.10 ± 0.12	3.12	Present work
15.0	11.6	97.18 ± 0.16	137.64 ± 0.09	3.18 ± 0.16	3.26	Present work
15.0	11.6	97.01 ± 0.08	137.80 ± 0.07	3.19 ± 0.12	3.26	[64]
17.3	12.71	97.02 ± 0.16	137.62 ± 0.09	3.37 ± 0.15	3.36	Present work
20.0	13.4	96.99 ± 0.07	137.61 ± 0.07	3.44 ± 0.11	3.47	[64]
25.0	14.38	96.84 ± 0.17	137.69 ± 0.18	3.47 ± 0.18	3.59	[62]
30.0	14.7	96.80 ± 0.08	137.64 ± 0.11	3.57 ± 0.11	3.62	[64]
35.0	15.08	96.74 ± 0.19	137.62 ± 0.19	3.64 ± 0.19	3.67	[59]
40.0	15.58	96.67 ± 0.13	137.72 ± 0.19	3.62 ± 0.19	3.73	[59]
48.0	16.22	96.64 ± 0.14	137.70 ± 0.15	3.66 ± 0.15	3.80	[52]
70.0	19.9	96.79 ± 0.07	137.55 ± 0.07	3.67 ± 0.11	4.23	[64]

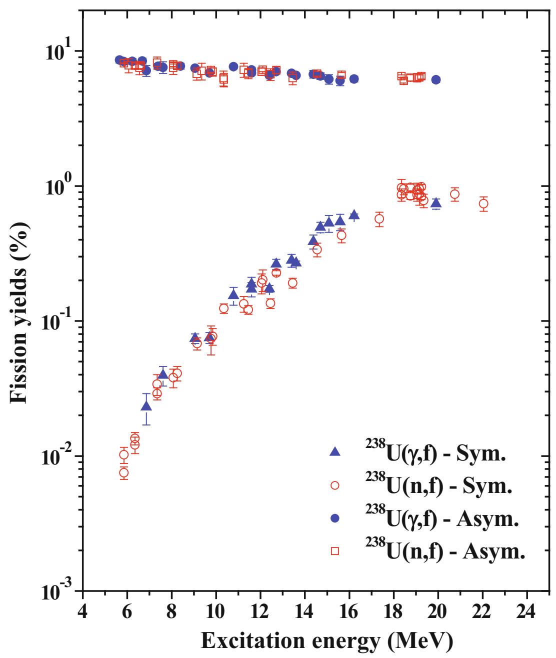

Fig. 6. Plot of the yields (%) of symmetric ($A = 115$–117) and asymmetric ($A = 133$–134) fission products as a function of the excitation energy in the bremsstrahlung- and neutron-induced fission of ^{238}U.

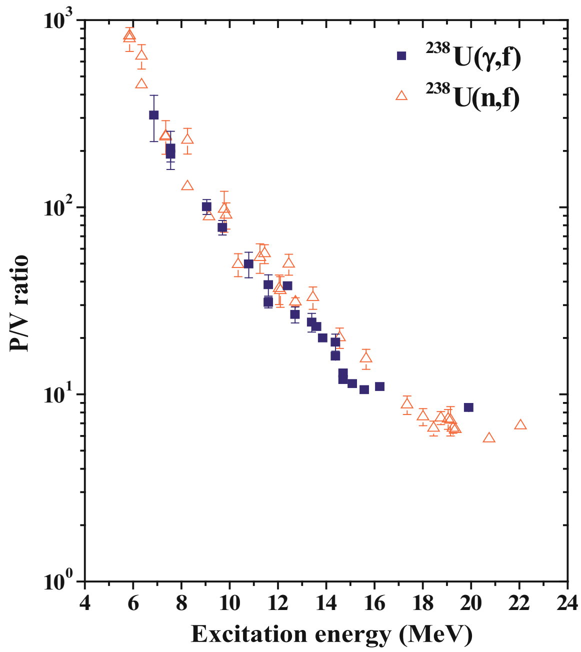

Fig. 7. Plot of the peak-to-valley (P/V) ratio as a function of the excitation energy in the bremsstrahlung- and neutron-induced fission of ^{238}U.

Table 10. Average light mass ($\langle A_L \rangle$), heavy mass ($\langle A_H \rangle$), and average neutron numbers ($\langle v \rangle_{expt}$) in the neutron-induced fission of ^{238}U.

E_n (MeV)	E^* (MeV)	$\langle A_L \rangle$	$\langle A_H \rangle$	$\langle v \rangle_{expt}$	Reference
1.5	5.85	97.5	139	2.5	[38]
2.0	6.35	97.5	139	2.5	[38]
3.72	8.07	97.44	138.89	2.67	[48]
3.9	8.25	97.4	138.9	2.7	[38]
5.42	9.77	97.27	138.82	2.91	[48]
5.5	9.85	97.4	138.6	3.0	[38]
6.9	11.51	97.5	138.4	3.1	[38]
7.7	11.05	97.4	138.3	3.3	[38]
7.75	12.1	97.37	138.33	3.31	[48]
8.1	12.45	97.48	138.13	3.39	[37]
9.1	13.45	97.4	138.06	3.6	[37]
10.09	14.55	97.37	138.03	3.6	[48]
14.8	19.15	98.0	136.8	4.2	[34]

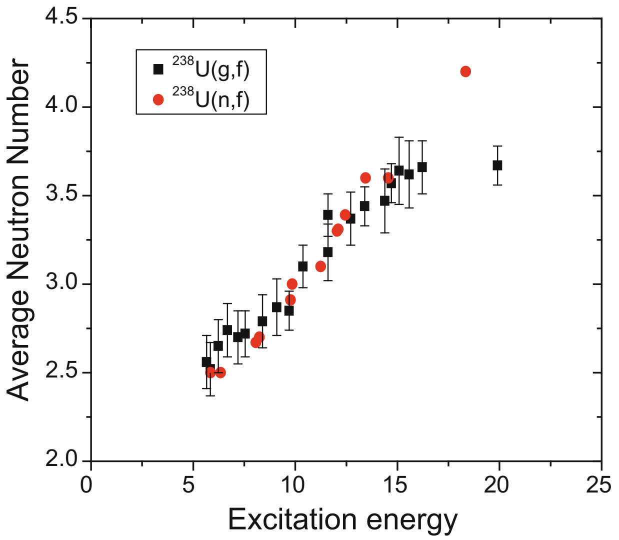

Fig. 8. Plot of the average neutron number($\langle v \rangle$) as a function of the excitation energy in the bremsstrahlung- and neutron-induced fission of ^{238}U.

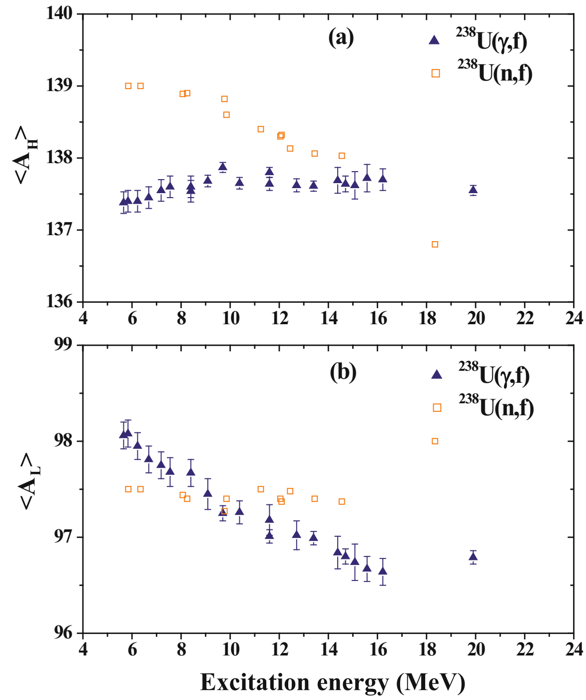

Fig. 9. Plot of the average values of the heavy mass ($\langle A_H \rangle$) and the average values of the light mass ($\langle A_L \rangle$) as a function of the excitation energy in the bremsstrahlung- and neutron-induced fission of ^{238}U.

Conclusions

i) The yields of the various fission products in the 11.5, 13.4, 15.0 and 17.3 MeV bremsstrahlung-induced fission of ^{238}U have been determined using the off-line gamma-ray spectrometric technique.

ii) In the bremsstrahlung- and neutron-induced fission of ^{238}U, the yields of the fission products around mass numbers 133–134, 139–140, 143–144 and their complementary products are higher than other fission products. This indicates the even-odd effect besides the role of shell closure proximity.

iii) The higher yields of the fission products around $A = 133$–134 and 143–144 and their complementary products are due to the presence of spherical $82n$ and deformed $88n$ shell. This is explainable from the point of standard I and standard II asymmetric mode of fission, which indicates the effect of shell closure proximity.

iv) The yields of the fission products around $A = 133$–134 and their complementary products are slightly higher in the ^{238}U(γ, f) reaction than in the ^{238}U(n, f) reaction. This is due to the presence of the spherical $82n$ and deformed $64n$ shell combination in the complementary fragment in the former than in the latter. The highest yield for $A = 133$–134 and 138–139 in the ^{238}U(γ, f) and ^{238}U(n, f) reactions is also favorable from the comparable N/Z ratio of the complementary fragments and fissioning systems besides the shell closure proximity.

v) It is a surprising fact that, with the increase of the excitation energy, the value of $\langle A_H \rangle$ slowly increases in the ^{238}U(γ, f) reaction but decreases significantly in the ^{238}U(n, f) reaction. On the other hand, with the increase of the excitation energy, the value of $\langle A_L \rangle$ decreases significantly in the ^{238}U(γ, f) reaction and increases slowly in the ^{238}U(n, f) reaction to conserve the mass of the fissioning system. This may be due to the different role of the standard I and II asymmetric modes of fission based on the shell combination of the complementary fragments and different types of potential energy surface between the ^{238}U(γ, f) and ^{238}U(n, f) reactions.

The authors express their sincere thanks to the staff of electron linac, SAPHIR, CEA, Saclay, France, for providing the electron beam to carry out the experiment. One of the authors (HN) thanks Mr. Pierre-Yves Thro and Mrs. Sylvie Aniel of International Division, CEA, Saclay, France, for providing financial support. HN also thanks Dr. K.L. Ramakumar, group director R&IC group for supporting the program and permitting him to visit the SAPHIR facility to carry out this experiment.

References

1. R. Vandenbosch, J.R. Huizenga, *Nuclear Fission* (Academic, New York, 1973).
2. C. Wagemans, *The Nuclear Fission Process* (CRC, London, 1990).
3. R.K. Sinha, A. Kakodkar, Nucl. Eng. Des. **236**, 683 (2006).
4. S. Ganesan, *Creation of Indian experimental benchmarks for thorium fuel cycle, IAEA Coordinated research project on "Evaluated data for thorium–uranium fuel cycle"*, in *Third Research Co-ordination Meeting, 30 January to 2 February 2006, Vienna, Austria, INDC (NDS)-0494* (2006).
5. F. Carminati, R. Klapisch, J.P. Revol, J.A. Rubia, C. Rubia, CERN/AT/93-49 (ET) 1993.
6. C. Rubia, J.A. Rubio, S. Buono, F. Carminati, N. Fietier, J. Galvez, C. Geles, Y. Kadi, R. Klapisch, P. Mandrilion, J.P. Revol, Ch. Roche, CERN/AT/95-44 (ET) 1995, CERN/AT/95-53(ET) 1995, CERN/LHC/96-01 (LET) 1996, CERN/LHC/97-01 (EET) 1997.
7. C.D. Bowman, AIP Conf. Proc. **346**, 22 (1994).
8. Accelerator Driven Systems: Energy Generation and Transmutation of NuclearWaste, Status report, IAEA, Vienna, IAEA-TECDO-985, Nov. 1997.
9. C.D. Bowman, Annu. Rev. Nucl. Part. Sci. **48**, 505 (1998).
10. S. Ganesan, Pramana, J. Phys. **68**, 257 (2007).
11. Fast Reactors and Accelerator Driven Systems Knowledge Base, IAEA-TECDOC-1319: Thorium fuel utilization: Options and Trends.
12. L. Mathieu *et al.*, *Proposition for a very simple Thorium Molten Salt reactor*, in *Proceedings of the Global International Conference*, Tsukuba, Japan, 2005 (2005) paper No. 428.
13. A. Nuttin, D. Heuer, A. Biliebaud, R. Brissot, C. Le Brun, E. Liatard, J.M. Loiseaux, L. Mathieu, O. Meplan, E. Merle-Lucotte, H. Nifenecker, F. Perdu, S. David, Proc. Nucl. Energy **46**, 77 (2005).
14. T.R. Allen, D.C. Crawford, *Lead-Cooled Fast Reactor Systems and the Fuels and Materials Challenges*, in *Science and Technology of Nuclear Installations*, (2007) 97486.
15. Annual Project Status Report 2000, MIT-ANP-PR-071, INEFL/EXT-2009-00994.
16. E.A.C. Crouch, At. Data Nucl. Data Tables **19**, 417 (1977).
17. B.F. Rider, *Compilation of fission products yields*, NEDO, 12154 3c ENDF-327, Valecicecitos Nuclear Centre, 1981.
18. J.R. England, B.F. Rider, *Evaluation and compilation of fission products yields*, ENDF/BVI, 1989, 1992.
19. M. James, R. Mills, *Neutron fission products yields*, UKFY2, 1991, JEF-2.2, 1993.
20. A.C. Wahl, At. Data Nucl. Data Tables **39**, 1 (1988).
21. H. Naik, A.G.C. Nair, P.C. Kalsi, A.K. Pandey, R.J. Singh, A. Ramaswami, R.H. Iyer, Radiochim. Acta **75**, 69 (1996).
22. R.H. Iyer, H. Naik, A.K. Pandey, P.C. Kalsi, R.J. Singh, A. Ramaswami, A.G.C. Nair, Nucl. Sci. Eng. **135**, 227 (2000).
23. K.M. Brown, Phys. Rev. **126**, 627 (1962).
24. M.P. Menon, P.K. Kurdo, J. Inorg. Nucl. Chem. **26**, 40 (1964).
25. N.L. Borisova, S.M. Dubrovina, V.I. Novgorodtseva, V.A. Pchelin, V.A. Shigin, V.M. Shubko, Sov. J. Nucl. Phys. **6**, 331 (1968).
26. D.J. Gorman, R.H. Tomilson, Can. J. Chem. **46**, 1663 (1968).
27. S.J. Lyle, J. Sellear, Radiochim. Acta **12**, 43 (1968).
28. S.J. Lyle, R. Wellum, Radiochim. Acta **13**, 167 (1969).
29. S.G. Birgul, S.J. Lyle, R. Wellum, Radiochim. Acta **16**, 104 (1971).
30. J.P. Bocquet, Nucl. Phys. **189**, 556 (1972).
31. D.R. Nethaway, B. Mendoza, Phys. Rev. C **6**, 1821, 1827 (1972).
32. J. Blachot, L.C. Carraz, P. Cavalini, C. Chauvin, A. Ferrieu, A. Moussa, J. Inorg. Nucl. Chem. **36**, 495 (1974).
33. J.T. Harvey, D.E. Adams,W.D. James, J.N. Beck, J.L. Meason, P.K. Kuroda, J. Inorg. Nucl. Chem. **37**, 2243 (1975).
34. D.E. Adams, W.D. James, J.N. Beck, P.K. Kuroda, J. Inorg. Nucl. Chem. **37**, 419 (1975).
35. M. Rajagopalan, H.S. Pruys, A. Grutter, E.A. Hermes, H.R. von Gunten, J. Inorg. Nucl. Chem. **38**, 351 (1976).
36. S. Daroczy, P. Raics, S. Naggy, L. Koever, I. Hamvas, E. Gorma, ATOMKI Kozl. **18**, 317 (1976).
37. T.C. Chapman, G.A. Anzelon, G.C. Spitale, D.R. Nethaway, Phys. Rev. C **17**, 1089 (1978).
38. S. Nagy, K.F. Flynn, J.E. Gindler, J.W. Meadows, L.E. Glendenin, Phys. Rev. C **17**, 163 (1978).
39. L. Wexin, S. Tongyu, Z. Manjiao, D. Tianrong, S. Xiuhua, He Huaxue, Yu F. Huakue, High Energy Phys. Nucl. Phys. **2**, 9 (1980) and **5**, 176 (1983).
40. L. Ze, Z. Chunhua, L. Conggui, W. Xiuzhi, Q. Limkun, C. Anzhi, L. Huijung, Z. Sujing, L. Yonghui, Ju Changxin, L. Daming, T. Peija, M. Jiangchen, J. Kixing, High Energy Phys. J. Nucl. Phys. **7**, 97 (1985).
41. L. Conggui, L. Huijun, L. Yonghui, (Chineese), High Energy Phys. Nucl. Phys. **7**, 235 (1985).
42. A. Afarideh, K.R. Annole, Ann. Nucl. Energy **16**, 313 (1989).
43. Z. Li, X. Wang, K. Jing, A. Cui, D. Liu, S. Su, P. Tang, T. Chih, S. Zhang, J. Gao, Radiochim. Acta **64**, 95 (1994).
44. G. Lhersonnau, P. Denloov, G. Canchel, J. Huikari, J. Jardin, A. Tokinen, V. KOlhinen, C. Lau, L. Lebroton, A.C. Mueller, A. Nieminen, S. Nummela, H. Penttila, K. Perajavi, Z. Radivojevic, V. Rubchenya, M.G. Saint-Laurent, W.H. Trzaska, D. Vakhtin, J. Vervier, A.C. Villari, J.C. Viang, J. Aystoe, Eur. Phys. J. A **9**, 385 (2000).
45. I. Clenk, Radiochim. Acta **85**, 85 (1999) and **89**, 481 (2001).
46. J. Laurec, A. Adam, T. DeBruyne, E. Brauge, T. Granier, J. Aupiais, O. Barsillon, G. Lepetit. N. Authier, P. Casoli, Nucl. Data Sheet **111**, 2965 (2010).
47. I.V. Ryzhov, S.G. Yavshits, G.A. Tutin, N.V. Kovalev, A.V. Saulski, N.A. Kudryashev, A.V. Saulski, N.A. Kudryashev, M.S. Onegin, L.A. Vaishnene, Yu.A. Gavrikov, O.T. Grudzevich, V.D. Simutkin, S. Pomp, J. Blomgren, M. Osterlund, P. Andersson, R. Bevilacqua, J. Meulders, R. Prieels, Phys. Rev. C **85**, 054603 (2011).

48. H. Naik, V.K. Mulik, P.M. Prajapati. B.S. Shivashankar, S.V. Suryanarayana, K.C. Jagadeesan, S.V. Thakare, S.C. Sharma, A. Goswami, Nucl. Phys. A **913**, 185 (2013).
49. K.-H. Schmidt, S. Steinhauser, C. Bockstiegel, A. Rewe, A. Heinz, A.R. Junghans, J. Benlliure, H.-G. Clerc, M. de Jong, J. Muller, M. Pfutzner, B. Voss, Nucl. Phys. A **665**, 211 (2000).
50. S. Steinhauser, J. Benlliure, C. Bockstiegel, H.-G. Clerc, A. Heinz, A. Rewe, M. de Jong, A.R. Junghans, J. Muller, M. Pfutzner, K.-H. Schmidt, Nucl. Phys. A **634**, 89 (1998).
51. J. Benlliure, A.R. Junghans, K.-H. Schmidt, Eur. Phys. J. A **13**, 93 (2002).
52. R.A. Schmitt, N. Sugarman, Phys. Rev. **95**, 1260 (1954).
53. H.G. Richter, C.D. Coryell, Phys. Rev. **95**, 1550 (1954).
54. L. Katz, T.M. Kavanagh, A.G.W. Cameron, E.C. Bailey, J.W.T. Spinks, Phys. Rev. **99**, 98 (1958).
55. J.L. Meason, P.K. Kuroda, Phys. Rev. **142**, 691 (1966).
56. I.R. Willams, C.B. Fulmer, G.F. Dell, M.J. Engebretson, Phys. Lett. B **26**, 140 (1968).
57. L.H. Gevaert, R.E. Jervis, S.C. Subbarao, H.D. Sharma, Can. J. Chem. **48**, 652 (1970).
58. B. Schrøder, G. Nydahl, B. Forkman, Nucl. Phys. A **143**, 449 (1970).
59. A. Chattopadhyay, K.A. Dost, I. Krajbich, H.D. Sharma, J. Inorg. Nucl. Chem. **35**, 2621 (1973).
60. D. Swindle, R. Wright, K. Takahashi, W.H. Rivera, L. Meason, Nucl. Sci. Eng. **52**, 466 (1973).
61. A. De Clercq, E. Jacobs, D. De Frenne, H. Thierens, P. D'hondt, A.J. Deruytter, Phys. Rev. C **13**, 1536 (1976).
62. H. Thierens, D. De Frenne, E. Jacobs, A. De Clercq, P. D'Hondt, A.J. Deruytter, Phys. Rev. C **14**, 1058 (1976).
63. W.D. James, D.E. Adams, R.A. Sigg, J.T. Harvey, J.L. Meason, J.N. Beck, P.K. Kuroda, H.L. Wright, J.C. Hogan, J. Inorg. Nucl. Chem. **38**, 1109 (1978).
64. E. Jacobs, H. Thierens, A. De Frenne, A. De Clercq, P. D'Hondt, P. De Gelder, A.J. Deruytter, Phys. Rev. C **19**, 422 (1979).
65. E. Jacobs, A. De Clercq, H. Thierens, D. De Frenne, P. D'hondt, P. De Gelder, A.J. Deruytter, Phys. Rev. C **20**, 2249 (1979).
66. E. Jacobs, H. Thierens, D. De Frenne, A. De Clercq, P. D'Hondt, P. De Gelder, A.J. Deruytter, Phys. Rev. C **21**, 237 (1980).
67. A. Yamadera, T. Kase, T. Nakamura, in *Proceedings of the International Conference on Nuclear Data for Science and Technology, Moto, Japan, 1988* (Japan Atomic Energy Research Institute, Tokai, Japan, 1988) p. 1147.
68. S. Pomme, E. Jacobs, K. Persyn, D. De Frenne, K. Govaert, M.L. Yoneama, Nucl. Phys. A **560**, 689 (1993).
69. S. Pomme, E. Jacobs, M. Piessens, D. De Frenne, K. Persyn, K. Govaert, N.-L. Yoneama, Nucl. Phys. A **572**, 237 (1994).
70. K. Persyn, E. Jacobs, S. Pomme, D. De Frenne, K. Govaert, M.-L. Yoneama, Nucl. Phys. A **615**, 198 (1997).
71. A. Gook, M. Chernykh, C. Eckardt, J. Enders, P. von Neumann-Cosel, A. Oberstedt, S. Oberestedt, A. Richter, Nucl. Phys. A **851**, 1 (2011).
72. H. Naik, V.T. Nimje, D. Raj, S.V. Suryanarayana, A. Goswami, S. Singh, S.N. Acharya, K.C. Mttal, S. Ganesan, P. Chandrachoodan, V.K. Manchanda, V. Venugopal, S. Banarjee, Nucl. Phys. A **853**, 1 (2011).
73. H. Naik, R.J. Singh, R.H. Iyer, Eur. Phys. J. A **16**, 495 (2003).
74. U. Brossa, S. Grossmann, A. Muller, Phys. Rep. **197**, 167 (1990).
75. B.D. Wilkins, E.P. Steinberg, R.R. Chasman, Phys. Rev. C **14**, 1832 (1976).
76. W.R. Nelson, H. Hirayama, D.W.O. Rogers, MAC report 265, 1985.
77. A.I. Blokhin, A.S. Soldatov, Phys. At. Nucl. **72**, 917 (2009).
78. J.T. Caldwell, E.J. Dowdy, B.L. Berman, R.A. Alvarez, P. Meyer, Phys. Rev. C **21**, 1215 (1980).
79. M. Veyssiere, H. Bell, R. Bergere, P. Carlos, A. Lepretre, K. Kernbath, Nucl. Phys. A **199**, 45 (1973).
80. E. Browne, R.B. Firestone, in *Table of Radioactive Isotopes*, edited by V.S. Shirley (Wiley, New York, 1986); and R.B. Firestone, L.P. Ekstrom, in *Table of Radioactive Isotopes*, Version 2.1 (2004) `http://ie.lbl.gov/toi/index.asp`.
81. J. Blachot, C. Fiche, Ann. Phys. Suppl. **6**, 3 (1981).
82. H. Umezawa, S. Baba, H. Baba, Nucl. Phys. A **160**, 65 (1971).
83. N. Sugarman, A. Turkevich, C.D. Coryell, N. Sugarman (Editors), in *Radiochemical Studies: The Fission Product* (McGraw-Hill, New York, 1951) p. 1396.
84. M. Strecker, R. Wein, P. Plischke, W. Scobel, Phys. Rev. C **41**, 2172 (1990).
85. C. Agarwal, A. Goswami, P.C. Kalsi, S. Singh, A. Mhatre, A. Ramaswami, J. Radioanal. Nucl. Chem. **275**, 445 (2008).
86. H. Naik, A. Goswami, G.N. Kim, M.W. Lee, K.S. Kim, S.V. Suryanarayana, E.A. Kim, M.-H. Cho, Phys. Rev. C **86**, 054607 (2012).
87. S. Bjornholm, J.E. Lynn, Rev. Mod. Phys. **52**, 725 (1980).
88. H. Nifenenecker, C. Signabieux, R. Babinet, J. Poitou, in *Physics and Chemistry of Fission*, Vol. **I** (IAEA, Vienna, 1973) p. 17.